A Game Theoretic Approach to Setting the Pilot Power Ratio in Multi-User MIMO Systems

Peiyue Zhao[†], Gábor Fodor[⋆†], György Dán[†], Miklós Telek[‡♯]
[†]KTH Royal Institute of Technology, Stockholm, Sweden. E-mail: {peiyue|gaborf|gyuri}@kth.se
[⋆]Ericsson Research, Stockholm, Sweden. E-mail: Gabor.Fodor@ericsson.com
[‡]Budapest University of Technology and Economics, Budapest, Hungary. E-mail: telek@hit.bme.hu
[♯]MTA-BME Information Systems Research Group, Budapest, Hungary. E-mail: telek@hit.bme.hu

***Abstract*—We consider the uplink of a single cell multi-user multiple input multiple output (MU-MIMO) system, in which the base station acquires channel state information at the receiver by means of uplink pilot signals. Since each mobile station has a sum power budget that is used to transmit pilot and data symbols, the pilot power ratio (PPR) has a large impact on the system performance in terms of spectral and energy efficiency. We formulate the problem of PPR setting as a non-cooperative game, in which each mobile station aims at minimizing the mean squared error of the uplink received data symbols at the base station. We show that in this game a unique Nash equilibrium exists, and propose an iterative decentralized algorithm – termed Best PPR Algorithm (BPA) – that is guaranteed to converge to that Nash equilibrium. Since BPA dynamically responds to the measured interference, it outperforms widely used schemes that use a predetermined PPR. BPA also performs close to the global optimum, especially when mobile stations with similar path loss values are co-scheduled in the MU-MIMO system. Based on these insights, we propose a practical signalling mechanism for implementing BPA in MU-MIMO systems.**

I. Introduction

In the uplink of multi-user multiple input multiple output (MU-MIMO) systems, the base station (BS) typically acquires channel state information (CSI) by means of uplink pilot or reference signals that are orthogonal in the code domain. For example, mobile stations (MSs) in long term evolution (LTE) systems use cyclically shifted Zadoff-Chu sequences to form demodulation reference signals allowing the BS to acquire channel state information at the receiver (CSIR), which is necessary for uplink data reception [1].

In general, in systems employing pilot aided channel estimation the number of pilot symbols and the pilot power ratio (PPR) play a crucial role in optimizing the system performance in terms of spectral and energy efficiency [2]–[6]. The seminal work by [2] evaluated the difference between the mutual information when the receiver has only an estimate of the channel and when it has perfect knowledge of the channel. It also established upper and lower bounds – related to the variance of the channel measurement error – on this difference. Subsequently, the results in [3] showed how training based channel estimation affects the capacity of the fading channel, recognizing that training imposes a substantial information-theoretic penalty, especially when the coherence interval T is only slightly larger than the number of transmit antennas M, or when the SNR is low. In these regimes, learning the entire channel is highly suboptimal. Conversely, if the SNR is high, and T is much larger than M, training-based schemes can come very close to achieving capacity. Therefore, the power that should be spent on training and data transmission depends on the relation between T and M. Subsequently, references [4], [5] established a lower bound specifically for multiple input multiple output (MIMO) orthogonal frequency division multiplexing (OFDM) systems with minimum mean squared error (MMSE) channel estimation. It was also shown that the optimal PPR that maximizes this lower bound or minimizes the average symbol error rate can increase the capacity by 10-20% as compared with a system using suboptimal PPR setting.

As the number of antennas and the number of simultaneously served users by a single BS increases, decentralized algorithms for MU-MIMO systems become important, because they help to reduce the required processing power. Therefore, there is an increasing interest in decentralized optimization schemes for MU-MIMO systems, see for example [7]–[10]. These papers either assume the availability of perfect CSI, or incorporate CSI errors, but do not address the joint optimization of setting the pilot and the data power. A different line of work proposed a game theoretic approach for decentralized power control and resource allocation in multi-user (MU) systems in which some form of "performance coupling" [11] exists among the users, as the increase of one user's performance degrades the performance of others, e.g., [12] and [13]. These references suggest that game theoretic approaches in MU systems are appealing, because they naturally admit decentralized algorithms that can be easily deployed by both network nodes and MSs. It is, however, unclear whether a game theoretic treatment could be used for designing low complexity decentralized algorithms for setting the PPR in MU cellular systems.

In this paper we address this problem. We propose a game theoretic approach to setting the PPR in the uplink (UL) of MU-MIMO systems and propose a decentralized algorithm that can be implemented in practice and converges to a unique Nash equilibrium. Thereby, the main contribution of the present paper is a decentralized MU (pilot and data) power allocation algorithm, which we refer to as Best pilot-to-data power ratio (PDPR) Algorithm (BPA). The numerical results obtained by testing BPA in a MU-MIMO system employing an increasing number of receive antennas yield several unique insights. Our results show that BPA performs close to the globally optimal

solution, which minimizes the sum of mean squared errors (MSEs) in MU-MIMO systems, and outperforms the traditional pilot power setting scheme that uses a fixed, predefined PPR.

The rest of the paper is organized as follows. Section II discusses related work and highlights the contributions of our paper with respect to these work. The subsequent section describes the system and channel estimation models. Section IV describes the receiver model and, for completeness, rewrites the closed form expression for the MSE of the uplink received data symbols as a function of the pilot and data transmit power levels. Section V derives the best response power allocation function that minimizes the MSE of the received data symbols. Based on the best response, we develop a decentralized algorithm called the BPA, which is executed by each MS and the BS in the system and, as its output, allocates transmit power to each MS. Section VI presents numerical results. Section VII concludes the paper.

II. Related Work and Contributions

Due to its central role in the performance of MIMO systems, many recent work investigated the performance impact of the PPR and proposed optimal or near-optimal schemes for setting the PPR [14]–[21]. The MU-MIMO scenario is analyzed in [14], in which the coherence interval of T symbols is spent for channel training, channel estimation, and precoder computation for downlink (DL) transmission. Specifically, the optimum number of terminals in terms of the DL spectral efficiency is determined for a given coherence interval, number of base station antennas, and signal-to-interference-plus-noise ratio (SINR). There is no receiver design involved and the pilot-to-data power trade-off is out of the scope of the considered optimization problem. The joint power loading of data and pilot symbols for the purpose of acquiring channel state information at the transmitter (CSIT) for precoding is considered in [15], but the impact of setting the PPR at the MU-MIMO receiver is not considered. In contrast, the UL sum-rate maximization problem by tuning the training period in a frequency-flat fading channel is considered in [18], without modeling the receiver structure at the BS. Reference [20] proposes a pilot design that maximizes the spectral efficiency of high mobility wireless communication systems that use pilot-assisted MMSE channel estimation. That work does not explicitly model the impact of CSI errors on MU-MIMO receivers, such as an MMSE receiver. Reference [16] investigated the optimization of the pilot overhead for single-user wireless fading channels, and the dependencies of this pilot overhead on various system parameters of interest (e.g. fading rate, SNR) were quantified. By finding an expansion of the spectral efficiency for the overhead optimization in terms of the fading rate around the perfect-CSI point, the square root dependence of both the overhead and the spectral efficiency penalty was clearly identified. More recently, references [17], [19], and [22] considered the uplink power control and PPR setting problem in MU-MIMO systems assuming practical (zero-forcing (ZF) and MMSE based) multiantenna receiver structures rather than using information theoretic capacity as a basis for performance evaluations. However, the papers mentioned above do not develop decentralized algorithms for PPR setting.

Another set of related papers develop decentralized optimization schemes for MIMO systems, either assuming the availability of perfect channel state information, or incorporating channel state information errors, but do not address the joint optimization of pilot and data power setting, see for example [7]–[10].

Also, a number of recent work proposed a game theoretic approach for power control and resource allocation in MU systems in which performance coupling exists among the users, as the increase of one user's performance degrades the performance of others [11], [23], [12], [13], [24], [25] and [26]. The MU power control problem for the Gaussian frequency-flat relay channel is modelled as a Gaussian interference relay game (GIRG) in [11]. In the GIRG, instead of allocating the power budget across the set of sub-channels, each player aims to decide the optimal power control strategy across a set of hops. For cooperative cognitive radio networks, a coalitional game theoretic approach is proposed in [23]. The coalitional game model captures a cooperative secondary spectrum access scenario, and involves primary and secondary spectrum users such that the secondary users can act as cooperative relays for the primary users. A non-cooperative feedback-rate control game with pricing is considered in [12], as a model of the downlink transmission of a closed-loop wireless network, in which a multi-antenna BS utilizes CSI feedback to properly set linear precoders to communicate with multiple users. Reference [13] proposes a distributed power splitting scheme for simultaneous wireless information and power transfer in relay interference channels, where multiple source-destination pairs communicate through energy harvesting relays. Authors in [24] model power control as a non-cooperative game between transmitter-receiver pairs and show the existence of equilibria using quasi-variational inequality theory. Reference [25] formulates the problem of downlink power control of small cell base stations under a total power constraint as a generalized Nash equilibrium problem and proves the existence of equilibria. The authors in [26] consider a game theoretical formulation of the improper graph multicoloring problem as a model of resource allocation between transmitter-receiver pairs, prove the existence of equilibria and provide polynomial complexity algorithms for computing equilibria.

A powerful game theoretic framework for the noncooperative maximization of mutual information assuming Gaussian interference channels in MU-MIMO systems is developed in [27]. As it is pointed out by [27], the main difficulty in the MIMO case as compared with single input single output (SISO) systems is that the optimal transmit directions of each MS change with the strategies of the other users, as opposed to the SISO case, where only the power allocation depends on the strategies of the other MSs. However, this framework assumes the availability of perfect CSI and does not address the trade-off between data transmission and channel estimation. In contrast, the work reported in [28] develops a game theoretic

approach to maximizing the own information rates subject to transmit power and robust interference constraints allowing for non-perfect CSI availability at the transmitters and receivers specifically in a cognitive radio environment. However, the aspect of tuning the pilot and data power levels subject to a sum power constraint is not considered. For the DL, reference [29] assumes perfect CSIT at the BS and proposes a partially asynchronous distributed algorithm based on a non-cooperative game to find the DL precoders in MU-MIMO systems.

Closest to our work is [21], which considers the problem of joint pilot and data power control for the MU-MIMO UL. However, the model of [21] uses a receiver that minimizes the MSE of the estimated data symbols only when perfect CSI is available. As it has been shown in our previous work [22], the performance of this *naive* receiver can be significantly improved by regularizing the receiver with respect to the statistics of the CSI estimation errors.

Thus, to the best of our knowledge, our paper is the first to propose dynamic and/or decentralized algorithms for setting the pilot-to-data power ratio in multi-user cellular systems based on game-theoretical foundations. Our main contribution is the decentralized PPR computation and the associated BPA algorithm, which incorporates several important and practically useful results. Specifically, the following are important parts of BPA:

- Proposition 2 shows that the MSE of a tagged MS is quasi-convex with respect to its data power and derives the unique MSE minimizer data power. This result is non-trivial, and interestingly, has not been derived previously in the literature. This result can be useful on its own for other research work in the area of multi-user MIMO receiver design and power allocation.
- We prove that a unique Nash equilibrium exists when the mobile stations use the above unique MSE minimizer as their best response function. This is a highly non-trivial result, whose proof involves a number of important steps, including Theorem 1, Lemmas 4-5, Proposition 3, and Theorem 2. Each of these steps, and especially the proof of Theorem 2, requires careful considerations that jointly lead to the practically useful BPA algorithm.
- The practical signalling mechanism proposed in Section VI helps the reader to put BPA into a system design context.

III. System and Channel Estimation Model

We consider the uplink of a MU-MIMO system, in which the MSs transmit orthogonal pilot sequences $\mathbf{s} = \left[s_1, ..., s_{\tau_p}\right]^T \in \mathbb{C}^{\tau_p \times 1}$, in which each pilot symbol is scaled as $|s_i|^2 = 1$, for $i = 1, .., \tau_p$. The pilot sequences are constructed such that they remain orthogonal as long as the number of spatially multiplexed users is maximum τ_p. Specifically, without loss of generality, we assume that the number of MU-MIMO MSs is $K \leq \tau_p$. In practice, $K \ll N_r$, where N_r is the number of antennas at the BS. Also, we use the $\mathcal{K} = \{1, \ldots, K\}$ set to denote the set of MSs.

We assume a frequency flat (narrow band) channel, within which the subcarriers can be considered having the same channel coefficient in the frequency domain. This is a realistic assumption considering, for example, a 3GPP LTE system based on OFDM, in which a channel (a physical resource block [1]) consists of 12 subcarriers corresponding to 180 kHz channel bandwidth, while the coherence bandwidth even in relatively large outdoor cells can be assumed to be at least $B_c = \frac{c}{\Delta} = 300$ kHz, where c is the speed of light and Δ is the maximum difference in length between different propagation paths from the transmitter to the receiver. Typical values for Δ are 30 meters (indoors) and 1000 meters (outdoors) [30, Chapter 2].

Specifically, given F subcarriers in the coherence bandwidth, a fraction of τ_p subcarriers are allocated to the pilot and $\tau_d \triangleq F - \tau_p$ subcarriers are allocated to the data symbols. Each MS may transmit using its full power budget P_{tot}, such the transmission power can be distributed unequally over the subcarriers. In particular, considering a transmit power $P^{(p)}$ for each pilot symbol and P for each data symbol, the sum constraint of

$$\tau_p P^{(p)} + \tau_d P = P_{tot} \tag{1}$$

is enforced, where $1 \leq \tau_p, \tau_d < F$. Thus, the $N_r \times \tau_p$ matrix of the received pilot signal from a specific MS at the BS can be conveniently written as:

$$\mathbf{Y}^p = \alpha\sqrt{P^{(p)}}\mathbf{h}\mathbf{s}^T + \mathbf{N}, \tag{2}$$

where we assume that $\mathbf{h} \in \mathbb{C}^{N_r \times 1}$ is a circular symmetric complex normal distributed column vector with mean vector $\mathbf{0}$ and covariance matrix $\mathbf{C}$ (of size N_r), denoted as $\mathbf{h} \sim \mathcal{CN}(\mathbf{0}, \mathbf{C})$, α accounts for the propagation loss, $\mathbf{N} \in \mathbb{C}^{N_r \times \tau_p}$ is the spatially and temporally additive white Gaussian noise (AWGN) with element-wise variance σ_p^2, where the index p refers to the noise power on the received pilot signal.

We assume that the BS uses either the least squares (LS) or the MMSE estimator to obtain an estimate of the channel at the receiver, and based on the below summarized results of [31] we show that our methodology to determine the MSE of the received data symbols is applicable in both cases.

A. LS Channel Estimation

For each MS, the BS utilizes pilot sequence orthogonality and estimates the channel based on (2) assuming:

$$\begin{aligned}\hat{\mathbf{h}}_{\text{LS}} &= \frac{1}{\alpha\sqrt{P^{(p)}}}\mathbf{Y}^p\mathbf{s}^*(\mathbf{s}^T\mathbf{s}^*)^{-1} = \mathbf{h} + \frac{1}{\alpha\sqrt{P^p}\tau_p}\mathbf{N}\,\mathbf{s}^* \\ &= \mathbf{h} + \frac{1}{\alpha\sqrt{P_{tot} - \tau_d P}\sqrt{\tau_p}}\mathbf{N}\,\mathbf{s}^*,\end{aligned} \tag{3}$$

where $\mathbf{s}^* = \left[s_1^*, ..., s_{\tau_p}^*\right]^T \in \mathbb{C}^{\tau_p \times 1}$ denotes the vector of pilot symbols, s^* denotes the complex conjugate of s, and $(\mathbf{s}^T\mathbf{s}^*) = \tau_p$. By considering $\mathbf{h} \sim \mathcal{CN}(\mathbf{0}, \mathbf{C})$, it follows that the estimated channel $\hat{\mathbf{h}}_{\text{LS}}$ is a circular symmetric complex normal distributed vector $\hat{\mathbf{h}}_{\text{LS}} \sim \mathcal{CN}(\mathbf{0}, \mathbf{R}_{\text{LS}})$, with

$$\mathbf{R}_{\text{LS}} \triangleq \mathbb{E}\{\hat{\mathbf{h}}_{\text{LS}}\hat{\mathbf{h}}_{\text{LS}}^H\} = \mathbf{C} + \frac{\sigma_p^2}{\alpha^2 P^{(p)}\tau_p}\mathbf{I}_{N_r}$$
$$= \mathbf{C} + \frac{\sigma_p^2}{\alpha^2(P_{tot}-\tau_d P)}\mathbf{I}_{N_r}. \quad (4)$$

B. MMSE Channel Estimation

In the case of MMSE channel estimation, it is useful to define the training matrix $\mathbf{S} = \mathbf{s} \otimes \mathbf{I}_{N_r}$ (of size $\tau_p N_r \times N_r$), so that $\mathbf{S}^H\mathbf{S} = \tau_p \mathbf{I}_{N_r}$ and the $\tau_p N_r \times 1$ vector of the received signal (2) can be conveniently rewritten as

$$\tilde{\mathbf{Y}}^p = \alpha\sqrt{P_p}\mathbf{S}\mathbf{h} + \tilde{\mathbf{N}},$$

where $\tilde{\mathbf{Y}}^p, \tilde{\mathbf{N}} \in \mathbb{C}^{\tau_p N_r \times 1}$.
The MMSE channel estimator aims at minimizing the MSE between the estimate $\hat{\mathbf{h}}_{\text{MMSE}} \triangleq \mathbf{H}\tilde{\mathbf{Y}}^p$ and the actual channel $\mathbf{h}$.

Lemma 1. *[10], [31] The optimal MMSE decoder is*

$$\mathbf{H} = \arg\min_{\mathbf{H}} \mathbb{E}\{||\mathbf{H}\tilde{\mathbf{Y}}^p - \mathbf{h}||_F^2\} =$$
$$= \alpha\sqrt{P^{(p)}}(\sigma_p^2\mathbf{I}_{N_r} + \alpha^2 P^{(p)}\mathbf{C}\mathbf{S}^H\mathbf{S})^{-1}\mathbf{C}\mathbf{S}^H,$$

where $\mathbf{H} \in \mathbb{C}^{N_r \times \tau_p N_r}$*, and the MMSE channel estimate is expressed as*

$$\hat{\mathbf{h}}_{\text{MMSE}} = \alpha\sqrt{P_p}(\sigma_p^2\mathbf{I}_{N_r} + \alpha^2 P_p\tau_p\mathbf{C})^{-1}\mathbf{C}\mathbf{S}^H(\alpha\sqrt{P_p}\mathbf{S}\mathbf{h} + \tilde{\mathbf{N}}) =$$
$$= \left(\frac{\sigma_p^2}{\alpha^2 P_p\tau_p}\mathbf{I}_{N_r} + \mathbf{C}\right)^{-1}\mathbf{C}\left(\mathbf{h} + \frac{1}{\alpha\sqrt{P_p}\tau_p}\mathbf{S}^H\tilde{\mathbf{N}}\right). \quad (5)$$

The covariance matrix of the estimated channel in the case of MMSE channel estimation is captured in the following lemma.

Lemma 2. *[31] The covariance matrix of the estimated channel with MMSE estimation is given as:*

$$\mathbf{R}_{\text{MMSE}} \triangleq \mathbb{E}\{\hat{\mathbf{h}}_{\text{MMSE}}\hat{\mathbf{h}}_{\text{MMSE}}^H\} \quad (6)$$
$$= \mathbf{C}^2 \cdot \left(\frac{\sigma_p^2}{\alpha^2(P_{tot}-\tau_d P)}\mathbf{I}_{N_r} + \mathbf{C}\right)^{-1}.$$

C. Conditional Distribution of the Channel

Equations (4) and (6) can be used to calculate the conditional distribution of the channels, which in turn plays an important role to determine the MSE of the uplink received data symbols.

Lemma 3. *[31] The conditional distribution of the channel given its estimation* $\hat{\mathbf{h}}$ *is*

$$(\mathbf{h}|\hat{\mathbf{h}}) \sim \mathcal{CN}(\mathbf{D}\hat{\mathbf{h}}, \mathbf{Q}), \quad (7)$$

where

$$\mathbf{D} = \begin{cases} \mathbf{C}\mathbf{R}_{\text{LS}}^{-1} & \textit{for LS estimation} \\ \mathbf{I}_{N_r} & \textit{for MMSE estimation} \end{cases}$$

$$\mathbf{Q} = \begin{cases} \mathbf{C} - \mathbf{C}\mathbf{R}_{\text{LS}}^{-1}\mathbf{C} & \textit{for LS estimation} \\ \mathbf{C} - \mathbf{R}_{\text{MMSE}} & \textit{for MMSE estimation} \end{cases}$$

with $\mathbf{R}_{\text{LS}}$ *and* $\mathbf{R}_{\text{MMSE}}$ *given in* (4) *and* (6)*, respectively.*

We emphasize here that for the subsequent optimal power allocation it has crucial importance that matrices $\mathbf{R}, \mathbf{D}, \mathbf{Q}$ of a given MS depend on its data power (due to (1)).

IV. Linear MMSE Receiver

A. Received Data Signal Model

The MU-MIMO received data signal at the BS can be written as:

$$\mathbf{y} = \underbrace{\alpha_\kappa \mathbf{h}_\kappa\sqrt{P_\kappa}x_\kappa}_{\text{User-}\kappa} + \underbrace{\sum_{k\neq\kappa}^{K}\alpha_k\mathbf{h}_k\sqrt{P_k}x_k}_{\text{Other users}} + \mathbf{n}_d, \quad (8)$$

where K is the number of users, $\alpha_k\mathbf{h}_k$ is the $M \times 1$ vector channel including large (α_k) and small scale ($\mathbf{h}_k$) fading between User-k and the BS, P_k is the data power per symbol of User-k, x_k is the transmitted data symbol by User-k and the notation $\mathbf{n}_d$ emphasizes the noise on the received data signal. We denote the row vector of the data power levels of the K MSs by $\mathbf{P} \triangleq \{P_1, \ldots, P_K\} \in \mathbb{R}^{1\times K}$.

B. Employing the Naive and the MMSE Receivers at the BS

We start by comparing the structures and resulting MSE expressions of two linear receivers.

Notice that when using the MMSE receiver, the MSE is a natural performance metric, since it is directly related to the objective function of the multi-user MIMO receiver. More importantly, several related works showed that in the case of the MMSE receiver, minimizing the MSE of the received data symbols is equivalent to maximizing the SINR of the received signal, and thereby maximizing the per-user data rate, see for example [32]–[34]. Moreover, as we shall see, in the case of a non-cooperative game, from each user's perspective, minimizing the MSE is a meaningful and useful basis for best response due to the above mentioned rate-MSE equivalence.

The naive receiver uses the estimated channel $\hat{\mathbf{h}}_\kappa$ as if it was the actual channel to estimate the data symbol transmitted by User-κ [35]:

$$\mathbf{G}_\kappa^{\text{naive}} = \alpha_\kappa\sqrt{P_\kappa}\hat{\mathbf{h}}_\kappa^H \cdot$$
$$\cdot \Big(\alpha_\kappa^2 P_\kappa\hat{\mathbf{h}}_\kappa\hat{\mathbf{h}}_\kappa^H + \underbrace{\sum_{k\neq\kappa}^{K}\alpha_k^2 P_k\mathbf{C}_k + \sigma_d^2\mathbf{I}}_{\substack{\text{MU-MIMO} \\ \text{interference plus noise}}}\Big)^{-1}, \quad (9)$$

where $\mathbf{G}_\kappa^{\text{naive}} \in \mathbb{R}^{1\times M}$ and it can be assumed that $\sigma_d^2 = \sigma_p^2$. This assumption is justified, because any subcarrier can be used for pilot and data symbols, and we assume AWGN on all subcarriers. In the sequel $\mathbf{G}_\kappa^{\text{naive}}$ and the associated $\text{MSE}^{\text{naive}}$ are used as a point of reference, because the naive receiver does not take into account the impact of channel estimation errors.

As it has been pointed out by [36]–[38], this above receiver structure needs to be regularized to obtain the MMSE receiver $\mathbf{G}_\kappa$ that minimizes the MSE of the received data symbols in the presence of CSI errors and takes into account the MU-MIMO interference:

$$\mathbf{G}_\kappa = \alpha_\kappa \sqrt{P_\kappa}\hat{\mathbf{h}}_\kappa^H \mathbf{D}_\kappa^H \cdot \tag{10}$$
$$\cdot \left(\alpha_\kappa^2 P_\kappa \left(\mathbf{D}_\kappa \hat{\mathbf{h}}_\kappa \hat{\mathbf{h}}_\kappa^H \mathbf{D}_\kappa^H + \mathbf{Q}_\kappa \right) + \underbrace{\sum_{k \neq \kappa}^{K} \alpha_k^2 P_k \mathbf{C}_k + \sigma_d^2 \mathbf{I}_{N_r}}_{\substack{\text{MU-MIMO} \\ \text{interference plus noise}}} \right)^{-1}.$$

Notice that in the case of a single user ($K = 1$) and perfect channel estimation, $\sigma_\kappa^2 = \sigma_d^2$, $\mathbf{D}_k = \mathbf{I}_{N_r}$, $\mathbf{Q}_k = \mathbf{0}$ and $\mathbf{G}_k^{\text{naive}} = \mathbf{G}_k$. In practice, the pilot and data power allocation is constrained such that for the data power levels $P_k \in \mathcal{P}_d = \left(0, \frac{P_{tot}}{\tau_d}\right) \ \forall k \in \{1, 2, ..., K\}$ hold, where τ_d (as well as τ_p) are identical for all users.

As a remark, set $\mathcal{P}_d$ has to be an open set, since (3) and (5) indicate that $\hat{\mathbf{h}}_{\text{LS}}$ and $\hat{\mathbf{h}}_{\text{MMSE}}$ are not defined for $P_\kappa = 0$, and (4) and (6) indicate that $\mathbf{R}_{\text{LS}}$ and $\mathbf{R}_{\text{MMSE}}$ are not defined for $P_\kappa = \frac{P_{tot}}{\tau_d}$. Therefore the MMSE receiver $\mathbf{G}_\kappa$ in (10) does not exist for $P_\kappa \in \{0, \frac{P_{tot}}{\tau_d}\}$. At the same time, setting the data power P_κ to zero or $\frac{P_{tot}}{\tau_d}$ means that no data symbol or no pilot symbol is transmitted, neither of which is of practical interest.

C. Determining the MSE With Identical Uncorrelated Receiver Antennas

In the case of proper antenna spacing, the channel covariance matrices can be modeled as $\mathbf{C}_\kappa = c_\kappa \mathbf{I}$, which by (4) and the definition of $\mathbf{D}_\kappa$ and $\mathbf{Q}_\kappa$ implies $\mathbf{R}_\kappa(\mathbf{P}) = r_\kappa(\mathbf{P}) \cdot \mathbf{I}$, $\mathbf{D}_\kappa(\mathbf{P}) = d_\kappa(\mathbf{P}) \cdot \mathbf{I}$, $\mathbf{Q}_\kappa(\mathbf{P}) = q_\kappa(\mathbf{P}) \cdot \mathbf{I}$, where the dependence of r_κ, d_κ and q_κ on $\mathbf{P}$ has been emphasized. Furthermore, $\mathbf{G}_\kappa^{\text{naive}} = g_\kappa^{\text{naive}} \cdot \hat{\mathbf{h}}_\kappa^H$, and $\mathbf{G}_\kappa = g_\kappa \cdot \hat{\mathbf{h}}_\kappa^H$, where:

$$g_\kappa^{\text{naive}}(\mathbf{P}) \triangleq \frac{\alpha_\kappa \sqrt{P_\kappa}}{\alpha_\kappa^2 P_\kappa ||\hat{\mathbf{h}}_\kappa||^2 + \underbrace{\sum_{k \neq \kappa}^{K} \alpha_k^2 P_k c_k + \sigma_d^2}_{\triangleq \sigma_\kappa^2(\mathbf{P}_{-\kappa})}}. \tag{11}$$

and

$$g_\kappa(\mathbf{P}) \triangleq \frac{\alpha_\kappa \sqrt{P_\kappa} d_\kappa}{\alpha_\kappa^2 P_\kappa \left(d_\kappa^2 ||\hat{\mathbf{h}}_\kappa||^2 + q_\kappa \right) + \underbrace{\sum_{k \neq \kappa}^{K} \alpha_k^2 P_k c_k + \sigma_d^2}_{\sigma_\kappa^2(\mathbf{P}_{-\kappa})}}, \tag{12}$$

where $\mathbf{P}_{-\kappa} \in \mathbb{R}^{1 \times (K-1)}$ denotes the power vector containing the transmit data powers of all except the κ-th MS. In the following, depending on the context, we interchangeably use the notation $\mathbf{P}$ and $(P_\kappa, \mathbf{P}_{-\kappa})$. Accordingly,

$$\sigma_\kappa^2 = \sigma_\kappa^2(\mathbf{P}_{-\kappa}) \triangleq \sum_{k \neq \kappa}^{K} \alpha_k^2 P_k c_k + \sigma_d^2 \tag{13}$$

captures the MU-MIMO interference to MS-κ plus noise as highlighted in (9) and (10). The short notation, σ_κ^2, is used occasionally for notational convenience. Notice that in a multi-user system, where $K \geq 2$, $\sigma_\kappa^2(\mathbf{P}_{-\kappa})$ is greater than the pilot noise power σ_p^2, since – according to (13) – $\sigma_\kappa^2(\mathbf{P}_{-\kappa})$ incorporates the multi-user interference in addition to the thermal noise. Furthermore, in this case, the MSE as a function of the estimated channel can be obtained as follows:

Proposition 1. *[22], [39] The unconditional MSE of the received data symbols of User-κ when the BS uses the naive and optimal $\mathbf{G}_\kappa$ receivers respectively are as follows.*

$$\begin{aligned} &\text{MSE}_\kappa^{\text{naive}}(\mathbf{P}) = \\ &d_\kappa^2 N_r \left(e^{\mu_\kappa^{\text{naive}}} \left(\mu_\kappa^{\text{naive}} + 1 + N_r \right) E_{in}\left(1 + N_r, \mu_\kappa^{\text{naive}}\right) - 1 \right) + \\ &+ \left(\frac{q_\kappa}{r_\kappa} + \mu_\kappa^{\text{naive}} \right) \left(e^{\mu_\kappa^{\text{naive}}} \left(\mu_\kappa^{\text{naive}} + N_r \right) E_{in}\left(N_r, \mu_\kappa^{\text{naive}}\right) - 1 \right) \\ &- 2 d_\kappa \cdot e^{\mu_\kappa^{\text{naive}}} N_r E_{in}\left(1 + N_r, \mu_\kappa^{\text{naive}}\right) + 1, \end{aligned} \tag{14}$$

$$\text{MSE}_\kappa(\mathbf{P}) = \mu_\kappa e^{\mu_\kappa} E_{in}\left(N_r, \mu_\kappa\right), \tag{15}$$

where $\mu_\kappa^{\text{naive}}$ and μ_κ, as functions of the data power vector $\mathbf{P}$, are defined by

$$\mu_\kappa^{\text{naive}} = \mu_\kappa^{\text{naive}}(\mathbf{P}) \triangleq \frac{\sigma_\kappa^2(\mathbf{P}_{-\kappa})}{\alpha_\kappa^2 P_\kappa r_\kappa(P_\kappa)}, \tag{16}$$

$$\text{and } \mu_\kappa = \mu_\kappa(\mathbf{P}) \triangleq \frac{q_\kappa(P_\kappa)\alpha_\kappa^2 P_\kappa + \sigma_\kappa^2(\mathbf{P}_{-\kappa})}{d_\kappa^2(P_\kappa)\alpha_\kappa^2 P_\kappa r_\kappa(P_\kappa)}. \tag{17}$$

$E_{in}(n, z) \triangleq \int_1^\infty \frac{e^{-zt}}{t^n}\, dt$ is a standard exponential integral function.

The proofs of the statements are provided in [39, Theorem 1] and [22, Lemma 2], respectively. Note that in (17), $\mu_\kappa(\mathbf{P})$ is continuous with respect to $P_\kappa \in \mathcal{P}_d$. Furthermore, as intuitively expected, in a MU-MIMO system with perfect channel estimation, that is, when $d_\kappa = 1$ and $q_\kappa = 0$, we have that $\mu_\kappa = \mu_\kappa^{\text{naive}}$, and the MSEs of the naive and MMSE receivers coincide, that is $\text{MSE}_\kappa = \text{MSE}_\kappa^{\text{naive}}$.

Notice that according to Proposition 1 $\text{MSE}_\kappa(\mathbf{P})$ depends on $q_\kappa(\mathbf{P})$, $d_\kappa(\mathbf{P})$ and $r_\kappa(\mathbf{P})$, which only depend on the second order statistics of the channel and the data power, by Lemma 2 and 3. Therefore, the $\text{MSE}_\kappa(\mathbf{P})$ is more sensitive to the path loss α_κ, and is less sensitive to the channel coherence time.

V. Decentralized Pilot Power Ratio Computation

In this section we develop a decentralized algorithm executed by the MSs based on concepts from non-cooperative game theory [40]. The key tenet of the proposed algorithm, which we call BPA, is that MSs iteratively update their PPRs such that the updated PPRs minimize their own MSEs, until the data power update falls below a predefined threshold. Notice that because of the power constraint in equation (1), setting the data power is equivalent to setting the PPR.

A. Best Response Power Allocation

As a first step, observe that $\text{MSE}_\kappa(\mathbf{P})$ given in (15) depends on the data power P_κ of MS-κ and on the data power allocation

$\mathbf{P}_{-\kappa}$ of the other MSs. For notational convenience, let us rewrite

$$\mathrm{MSE}_\kappa(\mathbf{P}) = \mathrm{MSE}_\kappa(P_\kappa, \mathbf{P}_{-\kappa}), \tag{18}$$

which makes this dependence explicit, and allows us to define the best response of MS-κ.

Definition 1. *The best response of MS-κ to the data power allocation $\mathbf{P}_{-\kappa}$ of the other MSs is a data power allocation $P_\kappa^\star$ that satisfies*

$$\mathrm{MSE}_\kappa(P_\kappa^\star, \mathbf{P}_{-\kappa}) \leq \mathrm{MSE}_\kappa(P_\kappa, \mathbf{P}_{-\kappa}),\ \forall P_\kappa \in \mathcal{P}_d. \tag{19}$$

Clearly, $P_\kappa^\star \in \mathcal{P}_d$, but for a given $\mathbf{P}_{-\kappa}$ the best response need not be unique in general. The following important result shows that in the PPR selection problem the best response is unique, and can be expressed in closed form.

Proposition 2. *For an arbitrary data power allocation $\mathbf{P}_{-\kappa} \in \mathcal{P}_d^{K-1}$, the function $\mathrm{MSE}_\kappa(\mathbf{P})$ is quasiconvex with respect to $P_\kappa \in \mathcal{P}_d$. Furthermore, $P_\kappa^\star(\mathbf{P}_{-\kappa})$ is the unique minimizer of $\mathrm{MSE}_\kappa(P_\kappa, \mathbf{P}_{-\kappa})$, where:*

$$P_\kappa^\star(\mathbf{P}_{-\kappa}) = \frac{P_{tot}}{\tau_d + \sqrt{\tau_d \frac{c_\kappa P_{tot} \alpha_\kappa^2 \frac{1}{\sigma_\kappa^2(\mathbf{P}_{-\kappa})} + \tau_d}{c_\kappa P_{tot} \alpha_\kappa^2 \frac{1}{\sigma_p^2} + 1}}}. \tag{20}$$

The proof of the proposition is given in the Appendix. Since the best response is unique, we use the notation $P_\kappa^\star(\mathbf{P}_{-\kappa})$ to denote the best response data power of MS-κ in the sequel.

From Proposition 2, the following corollary is immediate.

Corollary 1. *Under the constraint of the power budget in* (1)*, the pilot power allocation of MS-κ by its best response function is*

$$P_\kappa^{(p)^\star} = \frac{P_{tot} - \tau_d P_\kappa^\star(\mathbf{P}_{-\kappa})}{\tau_p}. \tag{21}$$

We are now ready to formulate the BPA algorithm.

B. The Best Pilot Power Ratio Algorithm

The proposed best PPR algorithm operates by iteratively computing the best response power allocation of each MS. The pseudo-code of the algorithm is shown in Algorithm 1. $P_\kappa^{(i)}$ denotes the data power computed by MS-κ in iteration i, which is the best response power allocation with respect to the data power $\mathbf{P}_{-\kappa}^{(i-1)}$ of the other MSs.

BPA takes two parameters as input: the MSE improvement threshold $\epsilon \geq 0$ and the mode of operation, which determines the initial data power.

If the mode of operation is MIN, then, MS-κ initializes its data power according to (20) in Line 2 of BPA assuming that the data power of the other MSs is zero, that is assuming $\mathbf{P}_{-\kappa} = \mathbf{0}$, where $\mathbf{0}$ is the vector of zeros of appropriate size. Although $\mathbf{P}_{-\kappa}$ cannot be set to zero in practice, MS-κ can initialize $P_\kappa^{(0)}$ using the assumption that $\mathbf{P}_{-\kappa} = \mathbf{0}$. Note that after executing Line 2 of BPA, $P_\kappa^{(0)} > 0$.

If the mode of operation is MAX, then, MS-κ initializes its data power according to (20) in Line 4 of BPA assuming that the data power of the other MSs is $\frac{P_{tot}}{\tau_d}\ \mathbf{e}$, where $\mathbf{e}$ is the vector of ones of appropriate size. Although $\mathbf{P}_{-\kappa}$ cannot be set to $\frac{P_{tot}}{\tau_d}\ \mathbf{e}$ in practice, MS-κ can initialize $P_\kappa^{(0)}$ using the assumption that $\mathbf{P}_{-\kappa} = \frac{P_{tot}}{\tau_d}\ \mathbf{e}$. Note that after executing Line 4 of BPA, $P_\kappa^{(0)} < \frac{P_{tot}}{\tau_d}$.

Algorithm 1: Best PPR Algorithm (BPA)

Input: MSE improvement threshold ϵ, Mode $\in \{\mathrm{MIN}, \mathrm{MAX}\}$

1 **if** *Mode* == MIN **then**
2 Initial data power $P_\kappa^{(0)} = P_\kappa^\star(\mathbf{0}),\ \forall \kappa \in \mathcal{K}$
3 **else**
4 Initial data power $P_\kappa^{(0)} = P_\kappa^\star\left(\frac{P_{tot}}{\tau_d}\ \mathbf{e}\right),\ \forall \kappa \in \mathcal{K}$
5 **end**
6 $i = 0$
7 **repeat**
8 BS sends σ_p^2 and $\sigma_\kappa^2\left(\mathbf{P}_{-\kappa}^{(i-1)}\right)$ to MS-κ, $\kappa \in \mathcal{K}$
9 **for** $\kappa \in \mathcal{K}$ **do**
10 **if then**
11 $P_\kappa^{(i)} = P_\kappa^\star\left(\mathbf{P}_{-\kappa}^{(i-1)}\right)$
12 **else**
13 $P_\kappa^{(i)} = P_\kappa^{(i-1)}$
14 **end**
15 **end**
16 $i = i + 1$
17 **until** $P_\kappa^{(i)} == P_\kappa^{(i-1)},\ \forall \kappa \in \mathcal{K}$;

Output: Data power allocation $\mathbf{P}$.

The initial setting in both modes ensures the convergence of BPA, as it will be shown in the proof of Theorem 1.

Then, in iteration i, all MSs compute their best response data powers according to equation (20) with the parameters (σ_p^2 and $\sigma_\kappa^2\left(\mathbf{P}_{-\kappa}^{(i-1)}\right)$) received from the BS. Recall from (13) that the $\mathbf{P}_{-\kappa}$ and AWGN are incorporated in $\sigma_\kappa^2(\mathbf{P}_{-\kappa})$, which is the received noise-plus-interference at the BS on the received signal of MS-κ. Furthermore, in practice, the BS continuously measures $\sigma_\kappa^2(\mathbf{P}_{-\kappa})$ [1], which would allow the smooth integration of BPA into the existing radio measurement and resource management algorithms executed by the BS.

If the MSE improvement $\mathrm{MSE}_\kappa\left(P_\kappa^{(i-1)}, \mathbf{P}_{-\kappa}^{(i-1)}\right) - \mathrm{MSE}_\kappa\left(P_\kappa^\star\left(\mathbf{P}_{-\kappa}^{(i-1)}\right), \mathbf{P}_{-\kappa}^{(i-1)}\right)$ exceeds the improvement threshold ϵ, MS-κ updates its data power $P_\kappa^{(i)}$ to $P_\kappa^\star\left(\mathbf{P}_{-\kappa}^{(i-1)}\right)$, otherwise it keeps its current data power. The algorithm terminates if no MS updates its data power in an iteration. Note that in BPA the MSs update their data powers simultaneously, which allows for a fast operation at the expense of maintaining synchronization among the MSs.

C. Fixed Point and Convergence of BPA

In this section, we show hat BPA converges to a data power allocation at the MSs such that the PPR of each MS corresponds to its best response to $\mathbf{P}_{-\kappa}$. In this allocation, no MS has an incentive to change its PPR, and, consequently,

BPA does not update the data power allocations, even when δ is set to zero.

In order to prove the existence of such an allocation, it is convenient to model the data power allocation problem as a non-cooperative strategic game (Chapter 2.1, [40]):

$$\mathcal{G} \triangleq < \mathcal{K}, (\mathcal{P}_d), (\mathrm{MSE}_\kappa(\mathbf{P})) >, \tag{22}$$

where the set of players is the set of MSs $\mathcal{K}$, the action set of MS-κ is the set of possible data power allocations $\mathcal{P}_d$, and the cost function of MS-κ is $\mathrm{MSE}_\kappa(\mathbf{P})$. Showing that there is a data power allocation from which no MS has an incentive to deviate is equivalent to showing that the game $\mathcal{G}$ has a pure strategy Nash equilibrium, defined as follows.

Definition 2. *For some $\epsilon \geq 0$ an ϵ-Nash equilibrium of the strategic game $\mathcal{G}$ is a data power allocation profile $\mathbf{P}$ such that for all $\kappa \in \mathcal{K}$*

$$\mathrm{MSE}_\kappa(P_\kappa, \mathbf{P}_{-\kappa}) \leq \mathrm{MSE}_\kappa(P'_\kappa, \mathbf{P}_{-\kappa}) + \epsilon, \ \forall P'_\kappa \in \mathcal{P}_d. \tag{23}$$

A pure strategy Nash equilibrium is an ϵ-Nash equilibrium for $\epsilon = 0$.

We can now state the following important property of $\mathcal{G}$.

Theorem 1. *BPA with $\epsilon = 0$ converges to a pure strategy Nash equilibrium of $\mathcal{G}$.*

Before we prove the theorem, let us recall that, by Proposition 2, the function $\mathrm{MSE}_\kappa(P_\kappa, \mathbf{P}_{-\kappa})$ is continuous and quasiconvex on $\mathcal{P}_d$. Since the action set $\mathcal{P}_d$ is an open set, it is not compact, and thus the basic results on Nash equilibrium existence do not hold (e.g., Theorem 1.2 in [41], [42]). To prove that even though the action set $\mathcal{P}_d$ is open, an equilibrium exists, we first formulate a monotonicity result on the best response function $P^\star_\kappa(\mathbf{P}_{-\kappa})$ as follows.

Lemma 4. *The best response function $P^\star_\kappa(\mathbf{P}_{-\kappa})$ of the data power for MS-κ is a strictly increasing function of the data power P_j $\forall j \in \mathcal{K} \setminus \kappa$.*

Proof. Taking the derivative of $P^\star_\kappa(\mathbf{P}_{-\kappa})$ with respect to P_j we obtain

$$\frac{\partial P^\star_\kappa(\mathbf{P}_{-\kappa})}{\partial P_j} = \frac{\partial P^\star_\kappa(\mathbf{P}_{-\kappa})}{\partial \sigma_\kappa(\mathbf{P}_{-\kappa})} \frac{\partial \sigma_\kappa(\mathbf{P}_{-\kappa})}{\partial P_j} =$$

$$= \frac{c_\kappa P_{tot}^2 U \alpha_\kappa^2 \alpha_j \sigma_\kappa(\mathbf{P}_{-\kappa}) \sqrt{UV\sigma_\kappa^2(\mathbf{P}_{-\kappa})\sigma_p^2\tau_d}}{V\left(U\sigma_\kappa^2(\mathbf{P}_{-\kappa})\tau_d + \sqrt{UV\sigma_\kappa^2(\mathbf{P}_{-\kappa})\sigma_p^2\tau_d}\right)^2}, \tag{24}$$

where $U = c_\kappa P_{tot}\alpha_\kappa^2 + \sigma_p^2$, and $V = c_\kappa P_{tot}\alpha_\kappa^2 + \sigma_\kappa^2(\mathbf{P}_{-\kappa})^2\tau_d$.

Observe that $\frac{\partial P^\star_\kappa(\mathbf{P}_{-\kappa})}{\partial P_j} > 0$, which shows that $P^\star_\kappa(\mathbf{P}_{-\kappa})$ is a strictly increasing function of the data power of the other MSs. Thus, the best response of MS-κ increases as the other MSs increase their data powers. □

In addition to Lemma 4, the following lemma will be useful for the proof of Theorem 1.

Lemma 5. *The best response function $P^\star_\kappa(\mathbf{P}_{-\kappa})$ of the data power for MS-κ is bounded by*

$$\underline{P_\kappa} \leq P^\star_\kappa(\mathbf{P}_{-\kappa}) < \overline{P_\kappa}, \tag{25}$$

where $\underline{P_\kappa} = \lim_{\Delta\to 0} P^\star_\kappa(\Delta\mathbf{e})$ and $\overline{P_\kappa} = \lim_{\Delta\to\infty} P^\star_\kappa(\Delta\mathbf{e})$. Furthermore, $0 < \underline{P_\kappa}$ and $\overline{P_\kappa} < \frac{P_{tot}}{\tau_d}$.

Proof. Because the best response $P^\star_\kappa(\mathbf{P}_{-\kappa})$ is strictly monotonically increasing in the data power P_j of the other MSs (by Lemma 4), it is sufficient to show that $\underline{P_\kappa}$ and $\overline{P_\kappa}$ exist by substitution into (20).

$$\underline{P_\kappa} = \lim_{\Delta\to 0} P^\star_\kappa(\Delta\mathbf{e}) = \frac{P_{tot}}{\tau_d + \sqrt{\tau_d \frac{\left(c_\kappa P_{tot}\alpha_\kappa^2 + \sigma_d^2\tau_d\right)\sigma_p^2}{\left(c_\kappa P_{tot}\alpha_\kappa^2 + \sigma_p^2\right)\sigma_d^2}}}, \tag{26}$$

from which $0 < \underline{P_\kappa}$.

$$\overline{P_\kappa} = \lim_{\Delta\to\infty} P^\star_\kappa(\Delta\mathbf{e}) = \frac{P_{tot}}{\tau_d + \sqrt{\frac{\tau_d^2\sigma_p^2}{c_\kappa P_{tot}\alpha_\kappa^2 + \sigma_p^2}}}. \tag{27}$$

Since the second term in the denominator is positive, it follows that $\overline{P_\kappa} < \frac{P_{tot}}{\tau_d}$. □

We note that $\lim_{\mathbf{P}_{-\kappa}\to\infty}$ is not feasible in practice since it is out of the action set $\mathcal{P}_d$, but it suffices for the purpose of the mathematical proof.

We are now ready to prove Theorem 1.

Proof. We use induction to show that BPA converges. The proof is presented for the case of $Mode = \mathrm{MIN}$; the proof for $Mode = \mathrm{MAX}$ is analogous.

Recall that BPA starts with the initial power allocation $P^{(0)}_\kappa = P^\star_\kappa(\mathbf{0})$, and after the first iteration we have $P^{(1)}_\kappa = P^\star_\kappa\left(\mathbf{P}^{(0)}_{-\kappa}\right)$. Since $\mathbf{P}^{(0)}_{-\kappa} > \mathbf{0}$, according to Lemma 4, we have $P^{(1)}_\kappa > P^{(0)}_\kappa$ for all $\kappa \in \mathcal{K}$.

Consider now iteration i, and assume that $\mathbf{P}^{(i)}_{-\kappa} > \mathbf{P}^{(i-1)}_{-\kappa}$, which holds for $i = 1$. Then, by Lemma 4 we have $P^{(i+1)}_\kappa > P^{(i)}_\kappa$, and $\mathbf{P}^{(i+1)}_{-\kappa} > \mathbf{P}^{(i)}_{-\kappa}$ for all $\kappa \in \mathcal{K}$. Thus, the sequence $\{P^{(i)}_\kappa\}$ is a strictly monotone increasing sequence.

To show convergence, recall that by Lemma 5, the best response data power satisfies

$$0 < \underline{P_\kappa} \leq P^\star_\kappa(\mathbf{P}_{-\kappa}) < \overline{P_\kappa} < \frac{P_{tot}}{\tau_d}$$

for each MS-κ, and thus the sequence is bounded. By the monotone convergence theorem, it is convergent, which proves the convergence of BPA. □

The above result shows that there is a data power allocation $\mathbf{P}^{(\infty)}$ to which BPA converges. We can now state the following proposition.

Proposition 3. *The strategic game $\mathcal{G}$ has a pure strategy Nash equilibrium. Specifically, the power allocation $\mathbf{P}^{(\infty)}$, to which BPA converges, is a pure strategy Nash equilibrium of $\mathcal{G}$ when $\epsilon = 0$.*

Proof. The BPA sets $P_\kappa^{(\infty)} = P_\kappa^\star\left(\mathbf{P}_{-\kappa}^{(\infty)}\right)$ and by Proposition 2 and Definition 1 for all $\kappa \in \mathcal{K}$, it holds that:

$$\mathrm{MSE}_\kappa\left(P_\kappa^{(\infty)}, \mathbf{P}_{-\kappa}^{(\infty)}\right) \leq \mathrm{MSE}_\kappa\left(P'_\kappa, \mathbf{P}_{-\kappa}^{(\infty)}\right) \forall P'_\kappa \in \mathcal{P}_d. \tag{28}$$

By Definition 2, $\mathbf{P}^{(\infty)}$ is a pure Nash equilibrium of the strategic game $\mathcal{G}$. □

Clearly, in practice BPA would be used with a MSE improvement threshold $\epsilon > 0$, and $\{P_\kappa^{(i)}\}$ is an increasing sequence with $P_k^{(i+1)} \geq P_k^{(i)} \ \forall i$. Thus, similarly to the proof of Theorem 1, BPA converges to an approximate Nash equilibrium when $\epsilon > 0$, as stated by the following observation.

Observation 1. *For $\epsilon > 0$, BPA converges to a ϵ-Nash equilibrium power allocation profile.*

D. Uniqueness of the Fixed Point of BPA

According to (20), the best response power allocation $P_\kappa^\star(\mathbf{P}_{-\kappa})$ of MS-κ is a function of the currently used transmit power of all other MSs. In this section we define $\mathbf{f} : \mathbb{R}^{1\times K} \mapsto \mathbb{R}^{1\times K}$ as a mapping from $\mathbf{P}$ to $\mathbf{P}^\star$ and prove that $\mathbf{f}$ is a contraction mapping in $\mathcal{P}_d^{1\times K}$ and consequently has a unique fixed point, and BPA converges to this unique fixed point, if an easy to check condition holds.
Define

$$\mathbf{f}(\mathbf{P}) \triangleq \left[P_1^\star(P_1, \mathbf{P}_{-1}), \ldots, P_K^\star(P_K, \mathbf{P}_{-K})\right], \tag{29}$$

where $P_\kappa^\star\left(P_\kappa, \mathbf{P}_{-\kappa}\right)$ is independent of P_κ. Furthermore, define the $K \times K$ matrix $\mathbf{F}(\mathbf{P})$ so that its $(i,j)^{th}$ element is:

$$\mathbf{F}(\mathbf{P})_{ij} \triangleq \frac{\partial}{\partial P_i} f_j(\mathbf{P}) = \frac{\partial}{\partial P_i} P_j^\star(\mathbf{P}), \tag{30}$$

where $f_j(\mathbf{P}) = P_j^\star(\mathbf{P}_{-j})$ denotes the j^{th} element of row vector $\mathbf{f}(\mathbf{P})$. Note that $\mathbf{F}(\mathbf{P})_{ii} = 0$.

Theorem 2. *The best response power allocation as defined by* (29) *is a contraction mapping if the following condition holds for $\forall\kappa$ and $\forall\mathbf{P} \in \mathcal{P}_d^{1\times K}$:*

$$\frac{P_{tot}}{\tau_d} \cdot \frac{c_\kappa \alpha_\kappa^2 \sqrt{u_\kappa \sigma_\kappa^2\left(\mathbf{P}_{-\kappa}\right)}}{2\left(\sqrt{u_\kappa \sigma_\kappa^2\left(\mathbf{P}_{-\kappa}\right)} + \sqrt{c_\kappa \alpha_\kappa^2 + \frac{\tau_d}{P_{tot}} \sigma_\kappa^2\left(\mathbf{P}_{-\kappa}\right)}\right)^2} \cdot$$
$$\cdot \frac{1}{\sqrt{c_\kappa \alpha_\kappa^2 + \frac{\tau_d}{P_{tot}} \sigma_\kappa^2\left(\mathbf{P}_{-\kappa}\right)} \cdot \sigma_\kappa^2\left(\mathbf{P}_{-\kappa}\right)} \cdot \sum_{k=1, k\neq\kappa}^{K} c_k \alpha_k^2 \leq \eta < 1, \tag{31}$$

where η is a number arbitrarily close to one and

$$u_\kappa \triangleq \frac{c_\kappa \alpha_\kappa^2 \tau_d}{\sigma_p^2} + \frac{\tau_d}{P_{tot}}.$$

The proof is in the Appendix.

Note that the condition stated in Theorem 2 is mild in the sense that it is always fulfilled in practice. This is illustrated in Table I, in which the parameters of a system of 10 users are shown. The last row of the Table shows the value that must be less than 1 for the uniqueness of the Nash equilibrium. In this example the condition could be violated by letting the power budget P_{tot} grow to $\sim 6 \cdot 10^6$ mW, which can clearly not be the case in practice.

Table I
NUMERICAL EXAMPLE FOR CONTRACTIVITY BASED ON (31)

Parameter or Expression	**Value**
K	10
$c_k, \ \forall k$	1
Path Loss $(\mathrm{PL})_k, \ \forall k$	42.5 dB
$\alpha_k = 10^{-\frac{\mathrm{PL}}{10}}, \ \forall k$	$5.6234 \cdot 10^{-5}$
τ_d	10
P_{tot}	24 dBm $\approx$ 250 mW
$P_k, \ \forall k$	200 mW
P_{tot}/τ_d	25 mW
$u_\kappa = \frac{c_\kappa \alpha_\kappa^2 \tau_d}{\sigma_p^2} + \frac{\tau_d}{P_{tot}}$	$4.0032 \cdot 10^{-2}$
$\sigma_\kappa^2 = \sum_{k\neq\kappa}^{K} c_k \alpha^2 P_k + \sigma_d^2$	$1.0057 \cdot 10^{-3}$
$U_\kappa \triangleq \sqrt{u_\kappa \sigma_\kappa^2}$	$6.3450 \cdot 10^{-3}$
$S_\kappa \triangleq \sqrt{c_\kappa \alpha_\kappa^2 + \frac{\tau_d}{P_{tot}} \sigma_\kappa^2}$	$6.3428 \cdot 10^{-3}$
$\mathrm{NUM} \triangleq c_\kappa \alpha_\kappa^2 \sqrt{u_\kappa \sigma_\kappa^2}$	$2.0065 \cdot 10^{-11}$
$\mathrm{DEN} \triangleq 2 \cdot (U_\kappa + S_\kappa)^2$	$3.2196 \cdot 10^{-4}$
$\frac{\mathrm{NUM}}{\mathrm{DEN}} \cdot \frac{1}{S_\kappa \cdot \sigma_\kappa^2}$	$9.7698 \cdot 10^{-3}$
$\sum_{k\neq\kappa}^{K} c_k \alpha_k^2$	$2.8461 \cdot 10^{-8}$
$\sum_{k=1}^{K} \frac{\partial P_\kappa^\star(\mathbf{P}_{-\kappa})}{\partial P_k}$	$6.9513 \cdot 10^{-9} \ll 1$

Recall from Proposition 3 that BPA converges to a Nash equilibrium. Since the best response power allocation is a contraction mapping, and BPA implements the best response power allocation, it follows that BPA converges to the fixed point of $\mathbf{f}$. The convergence to the fixed point and Proposition 3 imply that the fixed point is the unique Nash equilibrium.

VI. NUMERICAL RESULTS

In this section we consider a MU-MIMO system and present the numerical results. First, we verify the properties of the $\mathrm{MSE}_\kappa(\mathbf{P})$ and the best response function $P_\kappa^\star(\mathbf{P}_{-\kappa})$. Next, we analyze the convergence of BPA. Finally, we investigate

Table II
SYSTEM PARAMETERS

Parameter	**Value**
Number of antennas at the BS	$N_r = 8, \ldots, 80$
Number of MSs	$K = 2, 6$
Total number of symbols (per time slot)	$F = 12$
Number of data symbols (per time slot)	$\tau_d = 6$
Number of pilot symbols (per time slot)	$F - \tau_d$
Power budget	$P_{tot} = 24$ dBm
Thermal noise density	-174 dBm/Hz

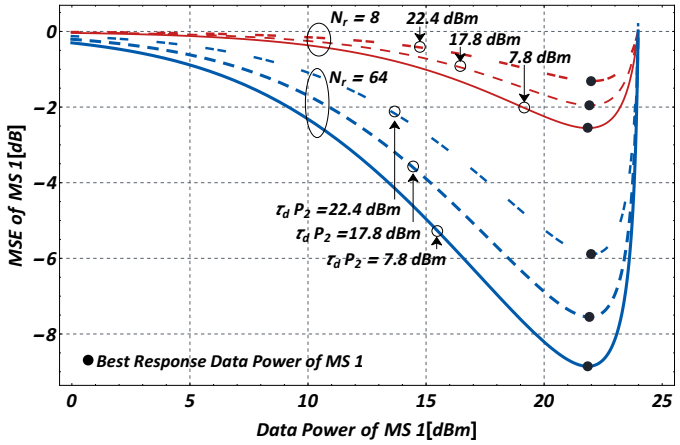

Figure 1. MSE of MS 1 as a function of data power of MS 1 in a two-MSs system. MSE_1 suffers from higher data power of MS 2 and benefits from deploying more antennas at the BS.

the performance of BPA in several scenarios, in which the number of MSs, and the number of antennas at BS vary. These scenarios are characterized in terms of the parameters listed in Table II.

A. Fundamental Properties of MSE

To examine fundamental properties of the $\mathrm{MSE}_\kappa(\mathbf{P})$ and the best response function $P_\kappa^\star(\mathbf{P}_{-\kappa})$, we first consider a system that consists of two MSs with fixed path loss values of $\alpha_1 = 50$ dB and $\alpha_2 = 42.5$ dB, respectively. Figure 1 shows the MSE performance of MS 1 as a function of the data power of MS 1 P_1, while setting $\tau_d P_2 = 7.8$ dBm, 17.8 dBm, and 22.4 dBm and employing $N_r = 8$ and $N_r = 64$ receive antennas at the BS. First, notice that the MSE of MS 1 is quasiconvex with respect to P_1. In all three cases of P_2, there exists a unique best response data power, which is marked by a dot in the figure. An important observation is that as the data power of MS 2 increases, the best response data power of MS 1 also increases. As an example, for the three cases of P_2 with $N_r = 8$, the best response data powers of MS 1 are 21.85 dBm, 21.93 dBm and 22.00 dBm, respectively.

Figure 2 shows the best response curves for a system of two MSs, that is when $K = 2$ in two cases. In case 1, we consider the same path loss allocation as those used in Figure 1. In case 2, the two MSs have equal path loss values of $\alpha_1 = \alpha_2 = 35$ dB. The curves show the best response data power for each MS with respect to the data power of the other MS. For example, in case 1, when $\tau_d P_1 = 21$ dBm, the best response of MS 2 is to use a data power level of $\tau_d P_2 \approx 22.4$dBm, since this data power level minimizes its own MSE. In both cases, MS 1 sets its data power as its best response to the current interference situation. Since the best response data power level increases with increasing interference power (that is with increasing P_2), MS 1 causes higher interference to MS 2. In turn, MS 2 increases its data power until they reach the Nash equilibrium point as illustrated by the intersection points in the figure. In consistence with the previous result, the best response data power increases as the data power of the other MS increases.

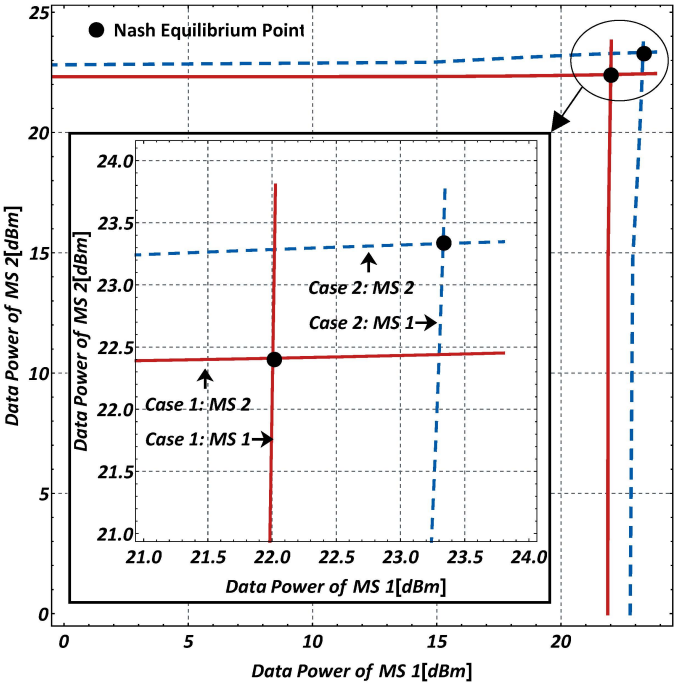

Figure 2. Illustration of the best response dynamics in a two-MSs system. The best response data power is an increasing function of the interference. The two MSs increase their data power until they reach a Nash equilibrium point.

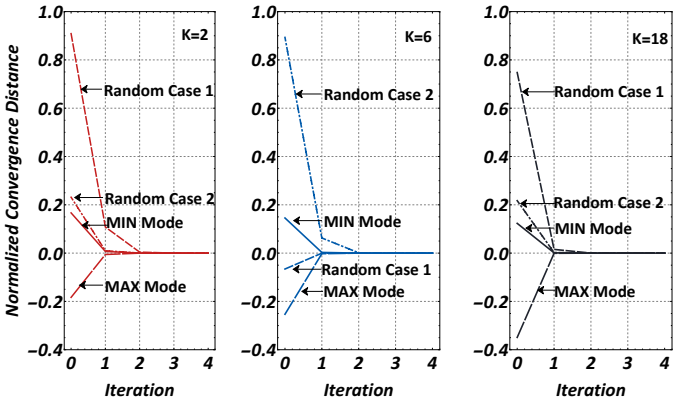

Figure 3. The normalized convergence distance in systems with 2, 6 and 18 MSs with different initial data power values. BPA converges within 4 iterations and the MIN mode has a shorter convergence distance.

B. Convergence of BPA

To evaluate the convergence of BPA, we define the normalized convergence distance $\mathrm{NCD}^{(i)}$ for each iteration as follows:

$$\mathrm{NCD}^{(i)} \triangleq \frac{\sum_{k\in\mathcal{K}} P_k^{(\infty)} - \sum_{k\in\mathcal{K}} P_k^{(i)}}{\sum_{k\in\mathcal{K}} P_k^{(\infty)}}, \qquad (32)$$

where $P_k^{(\infty)}$ is the data power of MS k in the Nash equilibrium. The algorithm converges as $\mathrm{NCD}^{(i)}$ approaches zero.

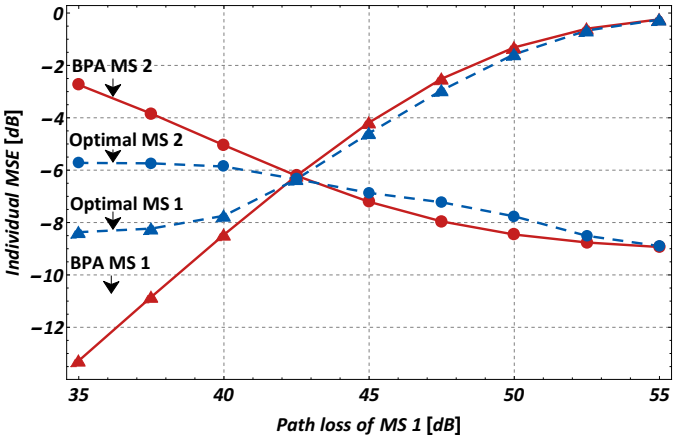

Figure 4. Individual MSE performance in a two-MSs system, where the path loss of MS 2 is fixed while the path loss of MS 1 is shown by the horizontal axis.

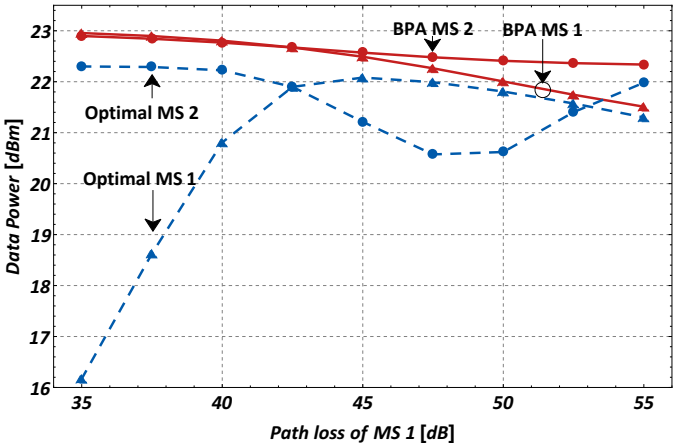

Figure 5. The individual data power levels of the two-MS system as set by BPA and in a system that minimizes the sum MSE.

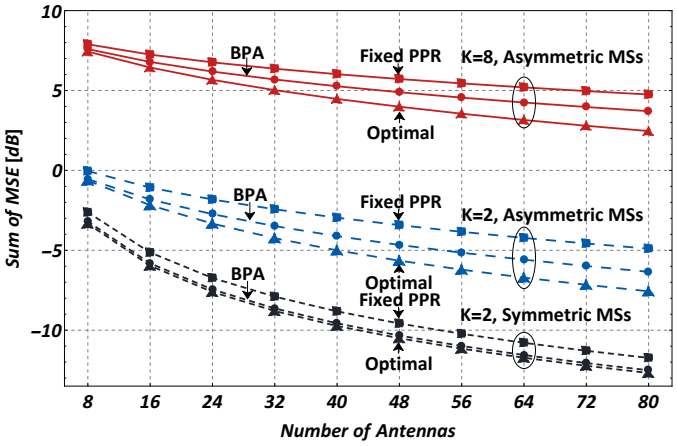

Figure 6. The sum-MSE performance in a system in which the co-scheduled MSs have equal or different path loss values when the BS is equipped with different number of antennas. BPA achieves near optimal sum-MSE performance in the system with symmetric (equal path loss) MSs, and outperforms the fixed PPR scheme.

Figure 3 shows the NCD for systems with $K = 2, 6$ and 18 MSs with BPA initialized in modes MIN and MAX, and for two cases when the data powers are chosen uniform at random. The results show that for all three system sizes BPA converges uniquely within four iterations, but the convergence performance of random initialization is unpredictable and hence randomly chosen data powers are not a good choice. For example, when there are 6 MSs the random case 1 has the largest convergence distance while the random case 2 has the shortest convergence distance. The results also show that after one iteration the convergence distance of MIN mode is lower than 0.02 for all three system sizes. This means that BPA achieves close-to-equilibrium performance and benefits the analyzed system already after a single iteration. In practical deployment one may thus apply the data power allocations obtained after a single iteration; such a solution would lead to close-to-equilibrium performance with very little overhead in terms of signaling traffic and in terms of delay. Since the MIN mode has a relatively shorter convergence distance than the MAX mode, we use the MIN mode in the rest of the simulations.

C. MSE Performance

To further evaluate the MSE performance of BPA, we compare its performance with that of a system that minimizes the sum of the individual MSEs. This minimum of the sum of the individual MSEs is obtained by *Mathematica* 10.0 [43] using exhaustive search.

We test BPA in a two-MSs system, as an extension of the scenario studied in Figure 1. The path loss of MS 2 is still fixed at 42.5 dB, while the path loss of MS 1 varies. Figure 4 shows the individual MSEs in different path loss settings of MS 1, while Figure 5 shows the corresponding data power levels. When using BPA, the MSs maximize their own MSE values at the expense of generating interference to the other MS, which has a negative impact on the overall system performance. When the path loss of the two MSs is different, both BPA and the system that minimizes the sum of the individual MSE values tend to be unfair in the sense of setting data power levels that yield unequal MSE values. For example, when MS 1 has lower path loss than MS 2 (e.g, $\alpha_1 = 35$ dB), the performance gap between the optimal and BPA is large. Due to the low path loss, MS 1 achieves a better MSE performance with BPA than with a sum-MSE minimizing algorithm. On the other hand, MS 2 suffers from the selfish behaviour of MS 1 in BPA. When the path loss values of the MSs are close to each other (e.g, $\alpha_1 = 40$ dB, 42.5 dB), the performance gap between BPA and optimal solution, and the performance gap between different MSs becomes smaller. When the path loss of MS 1 becomes large, MS 1 generates less interference, consequently the system performance is less sensitive to the interference, and the performance gap between the BPA and optimal solution remains small.

In currently deployed wireless systems, including LTE cellular networks, MU-MIMO schemes employ fixed (standardized) PPR setting for all MSs. Therefore, for benchmarking purposes, we simulate a regular scheme, which assigns $\frac{6}{7}P_{tot} \approx 23.31$ dBm power as the data transmission power for the MSs. This data power setting corresponds to the case of

using 6 out of 7 OFDM symbols for data transmission and 1 OFDM symbol for the pilot signal [1]. Figure 6 compares the performance of BPA with the optimal (i.e. sum-MSE minimizing) scheme and the regular scheme, when employing different number of antennas at the BS.

Figure 6 compares the performance of BPA with the optimal solution. For the system with 2 symmetric MSs (with equal path loss), the performance gap is always less than 0.5 dB. In a system with 2 MSs with different path losses (asymmetric setting), the performance gap of the two algorithms increases as the number of antennas increases. The largest gap is about 1.2 dB. A similar observation can be made for the system with 8 MSs. These results indicate that BPA performs close to the optimal solution when two MSs with similar path loss values are co-sheduled for MU-MIMO transmission. As expected, in all three cases, the system benefits from an increasing number of antennas at the BS.

As can also be seen in Figure 6, BPA outperforms the regular scheme with about $0.5 \sim 1$ dB in all three cases. The inferior performance of the regular scheme is due to using a fixed rather than adaptive data power. For example, in the system with 2 symmetric (equal path loss) MSs, the path loss values of the MSs are $\alpha_1 = \alpha_2 = 42.5$ dB. As Figure 5 shows in the two symmetric MSs case, BPA and the optimal solution set the data power as $\tau_d P_1 = \tau_d P_2 = 22.67$ dBm and $\tau_d P_1 = \tau_d P_2 = 21.89$ dBm, respectively. Since the regular scheme deploys unnecessarily high data power in this case, the performance suffers from high MU-MIMO interference.

D. A Practical Signalling Mechanism for BPA

In a real system, BPA can be performed periodically by the MSs assisted by a central entity such as a cellular BS. Based on the pseudo code description of Algorithm 1, we propose the following signalling mechanism for each PPR setting interval:

1) BS: broadcasts the data power update threshold δ, the mode of operation (i.e. MIN or MAX), and noise measurements σ_p^2, and σ_d^2 to the MSs.
2) Each MS: executes line 1-5 in BPA to initiate its data power $P_\kappa^{(0)}$.
3) BS: sends σ_p^2 and $\sigma_\kappa^2\left(\mathbf{P}_{-\kappa}^{(i-1)}\right)$ to each MS.
4) Each MS: executes line 10-14 in BPA to update its data power.
5) Repeat 3) and 4) until the system reaches the Nash equilibrium.

VII. Concluding Remarks

In this paper, we considered the uplink of a MU-MIMO system, in which the BS acquires CSIR by means of uplink pilot signals. Although it is well known, that in such systems setting the PPR for the MSs that are co-scheduled for uplink MU-MIMO transmission has a large impact on the performance, distributed PPR-setting schemes are not available in the literature. Given the growing interest in large scale antenna systems, there is a need for distributed schemes that scale well with both the number of receive antennas at the BS and the number of co-scheduled MU-MIMO users. This key observation motivated employing a game theoretic approach, in which MSs aim at minimizing the MSE of their own data symbols by adjusting their PPR under a fixed transmit power budget.

We first showed that there is a data power allocation at the MSs such that the PPR of each MS corresponds to its best response that minimizes its own MSE. We then developed a game theoretic decentralized algorithm – termed BPA – to set the PPR in MU-MIMO systems. Both the analytical and the numerical results showed the existence of a Nash equilibrium and the convergence of the proposed BPA to this equilibrium. We benchmarked BPA with respect to two reference schemes: the global optimum and a scheme that uses a fixed PPR.

The numerical results indicate that BPA converges after a few iterations even when the number of antennas and co-scheduled MU-MIMO users is set to realistic numbers. The achieved MSE performance is close to the global optimum that minimizes the sum of the individual MSE values when the co-scheduled users are similar in terms of large scale fading. Furthermore, BPA outperforms a PPR setting scheme that uses a predetermined (fix) pilot-data power ratio. We believe that these findings will be important in future MU-MIMO systems, in which distributed PPR setting schemes will be needed.

As a subject of future work, we plan to extend BPA to multi-cell MU-MIMO systems, in which the impact of pilot contamination on the quality of channel estimation must be taken into account.

Appendix: Proof of Proposition 2

The first derivative of the $\mathrm{MSE}_\kappa(\mathbf{P})$ with respect to P_κ is:

$$\frac{\partial \mathrm{MSE}_\kappa(\mathbf{P})}{\partial P_\kappa} = \frac{\partial \mathrm{MSE}_\kappa(\mathbf{P})}{\partial \mu_\kappa} \cdot \frac{\partial \mu_\kappa(\mathbf{P})}{\partial P_\kappa}. \tag{33}$$

>From [22, Appendix III], $\frac{\partial \mathrm{MSE}_\kappa(\mathbf{P})}{\partial \mu_\kappa}$ is positive $\forall \mu_\kappa(\mathbf{P}) > 0$. According to the power budget defined in equation (1), when $P_\kappa \in \mathcal{P}_d$, $P_{tot} - P_\kappa \tau_d > 0$ and thus $\mu_\kappa(\mathbf{P})$ is always positive. Thus the sign of $\frac{\partial \mathrm{MSE}_\kappa(\mathbf{P})}{\partial \mu_\kappa}$ in (33) only depends on the sign of $\frac{\partial \mu_\kappa(\mathbf{P})}{\partial P_\kappa}$.

$$\begin{aligned}\frac{\partial \mu_\kappa(\mathbf{P})}{\partial P_\kappa} = {} & \frac{1}{c_\kappa^2 P_\kappa^2 \alpha_\kappa^4 (P_{tot} - \tau_d P_\kappa)^2} \cdot \\ & \cdot \Big(\sigma_\kappa^2(\mathbf{P}_{-\kappa})\, \sigma_p^2 \big(2P_\kappa \tau_d - P_{tot}\big) + c_\kappa \alpha_\kappa^2 \cdot \\ & \cdot \Big(P_\kappa^2 \tau_d \big(\sigma_p^2 - \sigma_\kappa^2(\mathbf{P}_{-\kappa})\, \tau_d\big) + 2P_\kappa P_{tot} \sigma_\kappa^2(\mathbf{P}_{-\kappa})\, \tau_d - \\ & - \sigma_\kappa^2(\mathbf{P}_{-\kappa})\, P_{tot}^2 \Big) \Big).\end{aligned} \tag{34}$$

The denominator of (34) is positive. The numerator is a second order polynomial of P_κ with the coefficients $a_2 = c_\kappa \alpha_\kappa^2 \tau_d (\sigma_p^2 - \tau_d \sigma_\kappa^2(\mathbf{P}_{-\kappa}))$, $a_1 = 2\sigma_\kappa^2(\mathbf{P}_{-\kappa})\, \tau_d \left(c_\kappa \alpha_\kappa^2 P_{tot} + \sigma_p^2\right)$, and $a_0 = -P_{tot} \sigma_\kappa^2(\mathbf{P}_{-\kappa}) \left(c_\kappa P_{tot} \alpha_\kappa^2 + \sigma_p^2\right)$. According to the system

model, a_0 and a_2 are negative, and a_1 is positive. Thus the numerator of (34) has two positive roots $P^*_{\kappa,1}$ and $P^*_{\kappa,2}$:

$$P^*_{\kappa,1}=\frac{-a_1+\sqrt{a_1^2-4a_2a_0}}{2a_2}<P^*_{\kappa,2}=\frac{-a_1-\sqrt{a_1^2-4a_2a_0}}{2a_2}. \tag{35}$$

Comparison between the upper bound of the available data power of MS-κ and $P^*_{\kappa,2}$ indicates that

$$\frac{P_{tot}}{\tau_d}<\frac{P_{tot}}{\tau_d-\sqrt{\tau_d\frac{\left(c_\kappa P_{tot}\alpha_\kappa^2+\sigma_\kappa^2(\mathbf{P}_{-\kappa})\tau_d\right)\sigma_p^2}{\left(c_\kappa P_{tot}\alpha_\kappa^2+\sigma_p^2\right)\sigma_\kappa^2(\mathbf{P}_{-\kappa})}}}=P^*_{\kappa,2}. \tag{36}$$

Thus,

1) when $P_\kappa\in(0,P^*_{\kappa,1}]$, $\frac{\partial\mu_\kappa(\mathbf{P})}{\partial P_\kappa}$ and $\frac{\partial \mathrm{MSE}_\kappa(\mathbf{P})}{\partial P_\kappa}$ are negative,
2) when $P_\kappa\in[P^*_{\kappa,1},\frac{P_{tot}}{\tau_d})$, $\frac{\partial\mu_\kappa(\mathbf{P})}{\partial P_\kappa}$ and $\frac{\partial \mathrm{MSE}_\kappa(\mathbf{P})}{\partial P_\kappa}$ are positive.

$\mathrm{MSE}_\kappa(\mathbf{P})$ is continuous in $\mathcal{P}_d$, non-increasing in $(0,P^*_{\kappa,1}]$, and non-decreasing in $[P^*_{\kappa,1},\frac{P_{tot}}{\tau_d})$, thus $\mathrm{MSE}_\kappa(\mathbf{P})$ is quasiconvex with respect to P_κ in $\mathcal{P}_d$ (Chapter 3.4.2, [44]).

Further, as $P_\kappa=P^*_{\kappa,1}$ is the unique solution for $\frac{\partial \mathrm{MSE}_\kappa(\mathbf{P})}{\partial P_\kappa}=0$ in $\mathcal{P}_d$, $P^*_{\kappa,1}$ is the unique minimizer of $\mathrm{MSE}_\kappa(\mathbf{P})$, and

$$P^\star_{\kappa,1}=\frac{P_{tot}}{\tau_d+\sqrt{\tau_d\frac{\left(c_\kappa P_{tot}\alpha_\kappa^2+\sigma_\kappa^2(\mathbf{P}_{-\kappa})\tau_d\right)\sigma_p^2}{\left(c_\kappa P_{tot}\alpha_\kappa^2+\sigma_p^2\right)\sigma_\kappa^2(\mathbf{P}_{-\kappa})}}}. \tag{37}$$

Appendix: Proof of Theorem 2

We prove the theorem in two steps. First we show that $\mathbf{f}(\mathbf{P})$ is a contraction mapping on $\mathcal{P}_d^{1\times K}$ if its Fréchet derivative $\mathbf{F}(\mathbf{P})$ defined in (30) (i.e., the Jacobian) satisfies $||\mathbf{F}(\mathbf{P})||_1\le\eta<1$ on $\mathcal{P}_d^{1\times K}$, and then we show that this condition is in turn equivalent to (31).

For the first step we use the following two properties of the infinity norm and the Fréchet derivative. First, for an arbitrary vector $\mathbf{\Delta}$

$$||\mathbf{\Delta F(P)}||_\infty\le||\mathbf{\Delta}||_\infty||\mathbf{F(P)}||_1.$$

Second, for any small $\epsilon>0$ there exists a $\hat{\mathbf{\Delta}}(\mathbf{P},\epsilon)>\mathbf{0}$ such that $\forall\mathbf{\Delta}\le\hat{\mathbf{\Delta}}(\mathbf{P},\epsilon)$,

$$||\mathbf{f(P+\Delta)}-\mathbf{f(P)}||_\infty-||\mathbf{\Delta F(P)}||_\infty\le\epsilon||\mathbf{\Delta}||_\infty,$$

where the $<$ and $\le$ relations between vectors are defined as element-wise relations.

Using the above two properties, and assuming $\epsilon=(1-\eta)/2$ we obtain

$$\begin{aligned}&||\mathbf{f(P+\Delta)}-\mathbf{f(P)}||_\infty\le||\mathbf{\Delta F(P)}||_\infty+||\mathbf{\Delta}||_\infty(1-\eta)/2\\&\le||\mathbf{\Delta}||_\infty||\mathbf{F(P)}||_1+||\mathbf{\Delta}||_\infty(1-\eta)/2\\&\overset{(a)}{\le}||\mathbf{\Delta}||_\infty\eta+||\mathbf{\Delta}||_\infty(1-\eta)/2=||\mathbf{\Delta}||_\infty(1+\eta)/2\\&<||\mathbf{\Delta}||_\infty,\end{aligned} \tag{38}$$

where $(1+\eta)/2<1$ because $\eta<1$, and $||\mathbf{F(P)}||_1\le\eta$ is used in inequality (a). Thus, $\forall\mathbf{P}\in\mathcal{P}_d^{1\times K}$ there is a neigborhood given by $\hat{\mathbf{\Delta}}(\mathbf{P},(1-\eta)/2)$ where $\mathbf{f(P)}$ is a contraction mapping.

To conclude the first step of the proof, we now show that this relation extends to any two points $\mathbf{P},\mathbf{P}'\in\mathcal{P}_d^{1\times K}$. For this, let us first define $\hat{\mathbf{\Delta}}_{min}(\epsilon)=\inf_{\mathbf{P}\in\mathcal{P}_d^{1\times K}}\hat{\mathbf{\Delta}}(\mathbf{P},\epsilon)$ and $\mathbf{D}=\mathbf{P}'-\mathbf{P}$. Clearly, for any $\mathbf{D}$ there is a positive integer N such that $\frac{1}{N}\mathbf{D}\le\hat{\mathbf{\Delta}}_{min}((1-\eta)/2)$. Using these definitions, we can write

$$\begin{aligned}&||\mathbf{f(P+D)}-\mathbf{f(P)}||_\infty=\\&\left\|\sum_{n=1}^N\mathbf{f}(\mathbf{P}+\frac{n}{N}\mathbf{D})-\mathbf{f}(\mathbf{P}+\frac{n-1}{N}\mathbf{D})\right\|_\infty\le\\&\sum_{n=1}^N\left\|\mathbf{f}(\mathbf{P}+\frac{n}{N}\mathbf{D})-\mathbf{f}(\mathbf{P}+\frac{n-1}{N}\mathbf{D})\right\|_\infty\overset{(b)}{<}\\&\sum_{n=1}^N\frac{1+\eta}{2}||\frac{1}{N}\mathbf{D}||_\infty=\frac{1+\eta}{2}||\mathbf{D}||_\infty<||\mathbf{D}||_\infty,\end{aligned} \tag{39}$$

where inequality (b) follows from applying (38) with $\mathbf{\Delta}=\frac{1}{N}\mathbf{D}$, for points $\mathbf{P}+\frac{n-1}{N}\mathbf{D}$, where n goes from 1 to N. Note that (39) shows that if $||\mathbf{F(P)}||_1\le\eta$ on $\mathcal{P}_d^{1\times K}$ then $\mathbf{f(P)}$ is a contraction mapping on $\mathcal{P}_d^{1\times K}$.

For the second step of the proof observe that the condition

$$||\mathbf{F(P)}||_1=\max_j\sum_{i=1}^K|\mathbf{F(P)}_{ij}|\le\eta, \tag{40}$$

can be reformulated as:

$$\sum_{k=1}^K\frac{\partial P^\star_\kappa(\mathbf{P}_{-\kappa})}{\partial P_k}\le\eta,\quad\forall\kappa, \tag{41}$$

since according to the proof of Lemma 4, $\frac{\partial P^\star_\kappa(\mathbf{P}_{-\kappa})}{\partial P_j}>0$. The left hand side of (41) can be written as

$$\begin{aligned}\sum_{k=1}^K\frac{\partial P^\star_\kappa(\mathbf{P}_{-\kappa})}{\partial P_k}&=\frac{\partial P^\star_\kappa(\mathbf{P}_{-\kappa})}{\partial\sigma^2_\kappa(\mathbf{P}_{-\kappa})}\cdot\sum_{k=1}^K\frac{\partial\sigma^2_\kappa(\mathbf{P}_{-\kappa})}{\partial P_k}=\\&=\underbrace{\frac{\partial P^\star_\kappa(\mathbf{P}_{-\kappa})}{\partial\sigma^2_\kappa(\mathbf{P}_{-\kappa})}}_{\triangleq T_1}\cdot\underbrace{\sum_{k=1,k\neq\kappa}^K c_k\alpha_k^2}_{\triangleq T_2}.\end{aligned} \tag{42}$$

To calculate T_1, we find it convenient to rewrite $P^\star_\kappa(\mathbf{P}_{-\kappa})$ as follows:

$$\begin{aligned}P^\star_\kappa(\mathbf{P}_{-\kappa})&=\frac{P_{tot}/\tau_d}{1+\sqrt{\frac{\tau_d c_\kappa\alpha_\kappa^2P_{tot}\sigma_p^2+\tau_d^2\sigma_p^2\sigma_\kappa^2(\mathbf{P}_{-\kappa})}{\tau_d^2\left(c_\kappa\alpha_\kappa^2P_{tot}+\sigma_p^2\right)\sigma_\kappa^2(\mathbf{P}_{-\kappa})}}}=\\&=\frac{P_{tot}/\tau_d}{1+\sqrt{\frac{\frac{1}{\tau_d}c_\kappa\alpha_\kappa^2P_{tot}\sigma_p^2+\sigma_p^2\sigma_\kappa^2(\mathbf{P}_{-\kappa})}{\left(\frac{1}{\tau_d}c_\kappa\alpha_\kappa^2P_{tot}\tau_d+\sigma_p^2\right)\cdot\sigma_\kappa^2(\mathbf{P}_{-\kappa})}}}=\\&=\frac{P_{tot}/\tau_d}{1+\sqrt{y\left(\sigma_\kappa^2(\mathbf{P}_{-\kappa})\right)}},\end{aligned} \tag{43}$$

where we introduced:

$$y\Big(\sigma_\kappa^2\left(\mathbf{P}_{-\kappa}\right)\Big) \triangleq \frac{\frac{1}{\tau_d}c_\kappa\alpha_\kappa^2 P_{tot}\sigma_p^2+\sigma_p^2\sigma_\kappa^2\left(\mathbf{P}_{-\kappa}\right)}{\left(\frac{1}{\tau_d}c_\kappa\alpha_\kappa^2 P_{tot}\tau_d+\sigma_p^2\right)\cdot\sigma_\kappa^2\left(\mathbf{P}_{-\kappa}\right)} = \\ = \frac{c_\kappa\alpha_\kappa^2+\frac{\tau_d}{P_{tot}}\sigma_\kappa^2\left(\mathbf{P}_{-\kappa}\right)}{\left(\frac{c_\kappa\alpha_\kappa^2\tau_d}{\sigma_p^2}+\frac{\tau_d}{P_{tot}}\right)\sigma_\kappa^2\left(\mathbf{P}_{-\kappa}\right)} = \\ = \frac{c_\kappa\alpha_\kappa^2+\frac{\tau_d}{P_{tot}}\sigma_\kappa^2\left(\mathbf{P}_{-\kappa}\right)}{u_\kappa\sigma_\kappa^2\left(\mathbf{P}_{-\kappa}\right)}. \quad (44)$$

and

$$u_\kappa \triangleq \frac{c_\kappa\alpha_\kappa^2\tau_d}{\sigma_p^2}+\frac{\tau_d}{P_{tot}}. \quad (45)$$

With this notation, we can now calculate T_1:

$$\frac{\partial P_\kappa^\star(\mathbf{P}_{-\kappa})}{\partial\sigma_\kappa^2\left(\mathbf{P}_{-\kappa}\right)} = \frac{P_{tot}}{\tau_d}\cdot\frac{\partial}{\partial y\Big(\sigma_\kappa^2\left(\mathbf{P}_{-\kappa}\right)\Big)}\cdot \\ \cdot\frac{1}{1+\sqrt{y\Big(\sigma_\kappa^2\left(\mathbf{P}_{-\kappa}\right)\Big)}}\cdot\frac{\partial y\Big(\sigma_\kappa^2\left(\mathbf{P}_{-\kappa}\right)\Big)}{\partial\sigma_\kappa^2\left(\mathbf{P}_{-\kappa}\right)} = \\ = \frac{P_{tot}}{\tau_d}\cdot\frac{\partial}{\partial y\Big(\sigma_\kappa^2\left(\mathbf{P}_{-\kappa}\right)\Big)}\frac{1}{1+\sqrt{y\Big(\sigma_\kappa^2\left(\mathbf{P}_{-\kappa}\right)\Big)}}\cdot \\ \cdot\frac{\partial}{\partial\sigma_\kappa^2\left(\mathbf{P}_{-\kappa}\right)}\frac{c_\kappa\alpha_\kappa^2+\frac{\tau_d}{P_{tot}}\sigma_\kappa^2\left(\mathbf{P}_{-\kappa}\right)}{u_\kappa\sigma_\kappa^2\left(\mathbf{P}_{-\kappa}\right)} = \\ = \frac{P_{tot}}{\tau_d}\cdot\frac{-1}{2\Big(1+\sqrt{y\Big(\sigma_\kappa^2\left(\mathbf{P}_{-\kappa}\right)\Big)}\Big)^2\cdot\sqrt{y\Big(\sigma_\kappa^2\left(\mathbf{P}_{-\kappa}\right)\Big)}} \\ \cdot\frac{-c_\kappa\alpha_\kappa^2}{u_\kappa\sigma_\kappa^4\left(\mathbf{P}_{-\kappa}\right)} \\ = \frac{P_{tot}}{\tau_d}\cdot\frac{c_\kappa\alpha_\kappa^2}{2\cdot\left(1+\sqrt{\frac{c_\kappa\alpha_\kappa^2+\frac{\tau_d}{P_{tot}}\sigma_\kappa^2(\mathbf{P}_{-\kappa})}{u_\kappa\sigma_\kappa^2(\mathbf{P}_{-\kappa})}}\right)^2}\cdot \\ \cdot\frac{1}{\sqrt{\frac{c_\kappa\alpha_\kappa^2+\frac{\tau_d}{P_{tot}}\sigma_\kappa^2(\mathbf{P}_{-\kappa})}{u_\kappa\sigma_\kappa^2(\mathbf{P}_{-\kappa})}}\cdot u_\kappa\sigma_\kappa^4\left(\mathbf{P}_{-\kappa}\right)}. \quad (46)$$

>From (46), we finally get:

$$\frac{\partial P_\kappa^\star(\mathbf{P}_{-\kappa})}{\partial\sigma_\kappa^2\left(\mathbf{P}_{-\kappa}\right)} = \\ \frac{P_{tot}}{\tau_d}\cdot\frac{c_\kappa\alpha_\kappa^2\sqrt{u_\kappa\sigma_\kappa^2\left(\mathbf{P}_{-\kappa}\right)}}{2\left(\sqrt{u_\kappa\sigma_\kappa^2\left(\mathbf{P}_{-\kappa}\right)}+\sqrt{c_\kappa\alpha_\kappa^2+\frac{\tau_d}{P_{tot}}\sigma_\kappa^2\left(\mathbf{P}_{-\kappa}\right)}\right)^2}\cdot \\ \cdot\frac{1}{\sqrt{c_\kappa\alpha_\kappa^2+\frac{\tau_d}{P_{tot}}\sigma_\kappa^2}\cdot\sigma_\kappa^2\left(\mathbf{P}_{-\kappa}\right)}. \quad (47)$$

Substituting this expression into T_1 of (42) we obtain the statement of the theorem.

REFERENCES

[1] S. Sesia, I. Toufik, and M. Baker, *LTE - The UMTS Long Term Evolution: From Theory to Practice*. WILEY, 2nd edition, 2011, ISBN-10: 0470660252.

[2] M. Médard, "The Effect upon Channel Capacity in Wireless Communications of Perfect and Imperfect Knowledge of the Channel," *IEEE Trans. on Information Theory*, vol. 46, no. 3, pp. 933–946, May 2000.

[3] B. Hassibi and B. M. Hochwald, "How Much Training is Needed in Multiple-Antenna Wireless Links ?" *IEEE Trans. on Information Theory*, vol. 49, no. 4, pp. 951–963, April 2003.

[4] T. Kim and J. G. Andrews, "Optimal Pilot-to-Data Power Ratio for MIMO-OFDM," *IEEE Globecom*, pp. 1481–1485, Dec. 2005.

[5] ——, "Balancing Pilot and Data Power for Adaptive MIMO-OFDM Systems," *IEEE Globecom*, 2006.

[6] T. Marzetta, "Noncooperative Cellular Wireless with Unlimited Numbers of Base Station Antennas," *IEEE Trans. Wireless Comm.*, vol. 9, no. 11, pp. 3590–3600, 2010.

[7] M. Ding and S. D. Blostein, "Relation Between Joint Optimizations for Multiuser MIMO Uplink and Downlink with Imperfect CSI," in *IEEE Intl. Conf. on Acoustics, Speech and Signal Processing (ICASSP)*, Mar. 2008, pp. 3149 – 3152.

[8] J. Kron, D. Persson, M. Skoglund, and E. G. Larsson, "Closed-Form Sum-MSE Minimization for the Two-User Gaussian MIMO Broadcast Channel," *IEEE Communications Letters*, vol. 15, no. 9, pp. 950–952, Sep. 2011.

[9] J. Wang, M. Bengtsson, B. Ottersten, and D. Palomar, "Robust MIMO Precoding for Several Classes of Channel Uncertainty," *IEEE Trans. Signal Processing*, vol. 61, no. 12, pp. 3056–3070, April 2013.

[10] H. Yin, D. Gesbert, M. Filippou, and Y. Liu, "A Coordinated Approach to Channel Estimation in Large-Scale Multiple-Antenna Systems," *IEEE Journal on Selected Areas in Communications*, vol. 31, no. 2, pp. 264–273, Feb. 2013.

[11] Y. Shi, J. Wang, K. B. Letaief, and R. K. Mallik, "A Game-Theoretic Approach for Distributed Power Control in Interference Relay Channels," *IEEE Trans. On Wireless Communications*, vol. 8, no. 6, pp. 3151–3161, 2009.

[12] L. Song, Z. Han, Z. Zhang, and B. Jiao, "Non-Cooperative Feedback-Rate Control Game for Channel State Information in Wireless Networks," *IEEE Journal on Selected Areas in Communications*, vol. 30, no. 1, pp. 188–197, 2012.

[13] H. Chen, Y. Li, Y. Jiang, Y. Ma, and B. Vucetic, "Distributed Power Splitting for SWIPT in Relay Interference Channels Using Game Theory," *IEEE Trans. On Wireless Communications*, vol. 14, no. 1, pp. 410–420, 2015.

[14] T. Marzetta, "How Much Training is Needed for Multiuser MIMO ?" *IEEE Asilomar Conference on Signals, Systems and Computers (ACSSC)* , pp. 359–363, Jun. 2006.

[15] C. P. Sukumar and R. M. M. Eltawil, "Joint Power Loading of Data and Pilots in OFDM Using Imperfect Channel State Information at the Transmitter," in *IEEE Global Communications Conference*, Nov. 2008, pp. 1–5.

[16] N. Jindal and A. Lozano, "A Unified Treatment of Optimum Pilot Overhear in Multipath Fading Channels," *IEEE Trans. on Communications*, vol. 58, no. 10, pp. 2939–2948, October 2010.

[17] K. Min, M. Jung, T. Kim, Y. Kim, J. Lee, and S. Choi, "Pilot Power Ratio for Uplink Sum-Rate Maximization in Zero-Forcing Based MU-MIMO Systems with Large Number of Antennas," in *IEEE Vehicular Technology Conference (VTC-Fall)*, Sep. 2013, pp. 1–5.

[18] K. T. Truong, A. Lozano, and R. W. H. Jr., "Optimal Training in Continuous Block-Fading Massive MIMO Systems," 20^{th} *European Wireless, Barcelona, Spain*, May 2014.

[19] K. Guo, Y. Guo, G. Fodor, and G. Ascheid, "Uplink Power Control with MMSE Receiver in Multi-Cell MU-Massive-MIMO Systems," in *Proc. of IEEE International Conference on Communications (ICC)*, Jun. 2014, pp. 5184–5190.

[20] N. Sun and J. Wu, "Maximizing Spectral Efficiency for High Mobility Systems with Imperfect Channel State Information," *IEEE Trans. Wireless Communication*, vol. 13, no. 3, pp. 1462–1470, March 2014.

[21] K. Guo, Y. Guo, and G. Ascheid, "Energy-Efficient Uplink Power Allocation in Multi-Cell MU-Massive-MIMO Systems," in *Proc. of European Wireless*, May 2015, pp. 1–5.

[22] G. Fodor, P. D. Marco, and M. Telek, "On the Impact of Antenna Correlation and CSI Errors on the Pilot-to-Data Power Ratio," *IEEE Trans. on Communications*, vol. 64, no. 6, pp. 2622 – 2633, April 2016.

[23] D. Li, Y. Xu, X. Wang, and M. Guizani, "Coalitional Game Theoretic Approach for Secondary Spectrum Access in Cooperative Cognitive Radio Networks," *IEEE Trans. On Wireless Communications*, vol. 10, no. 3, pp. 844–855, 2011.
[24] I. Stupia, L. Sanguinetti, G. Bacci, and L. Vandendorpe, "Power control in networks with heterogeneous users: A quasi-variational inequality approach," *IEEE Trans. Signal Process.*, vol. 63, no. 21, pp. 5691–5705, Nov. 2015.
[25] J. Wang, W. Guan, Y. Huang, R. Schober, and X. You, "Distributed optimization of hierarchical small cell networks: A gnep framework," *IEEE J. Sel. Areas Commun.*, vol. 35, no. 2, pp. 249–264, Feb. 2017.
[26] V. Pacifici and G. Dán, "Convergence in player-specific graphical resource allocation games," *IEEE J. Sel. Areas Commun.*, vol. 30, no. 11, pp. 2190–2199, Dec. 2012.
[27] G. Scutari, D. P. Palomar, and S. Barbarossa, "Competitive Design of Multiuser MIMO Systems Based on Game Theory: A Unified View," *IEEE Journal on Selected Areas in Communications*, vol. 26, no. 7, pp. 1089–1103, Aug. 2008.
[28] J. Wang, G. Scutari, and D. P. Palomar, "Robust MIMO Cognitive Radio Via Game Theory," *IEEE Trans. on Signal Processing*, vol. 59, no. 3, pp. 1183–1201, Mar. 2011.
[29] B. Fallah, B. X. Huang, and L. Tu, "Distributed Asynchronous Game Theoretic Solutions for Precoding Strategies in Multiuser MIMO Systems," *International Journal of Distributed and Parallel Systems (IJDPS)*, vol. 3, no. 4, pp. 133–143, July 2012.
[30] T. L. Marzetta, E. G. Larsson, H. Yang, and H. Q. Ngo, *Fundamentals of Massive MIMO*, T. L. Marzetta, Ed. Cambridge University Press, 2016, ISBN 1107175577.
[31] G. Fodor, P. D. Marco, and M. Telek, "Performance Analysis of Block and Comb Type Channel Estimation for Massive MIMO Systems," in *First International Conference on 5G for Ubiquitous Connectivity (5GU)*, Nov. 2014, pp. 62–69.
[32] P. Viswanath, V. Anantharam, and D. N. C. Tse, "Optimal Sequences, Power Control, and User Capacity of Synchronous CDMA Systems with Linear MMSE Multiuser Receivers," *IEEE Trans. on Information Theory*, vol. 45, no. 6, pp. 1968–1983, Sep. 1999.
[33] S. S. Christensen, R. Agarwal, E. de Carvalho, and J. M. Cioffi, "Weighted sum-rate maximization using weighted MMSE for MIMO-BC beamforming design," *IEEE Trans. on Wireless Communications*, vol. 7, no. 12, pp. 4792–4799, Dec. 2008.
[34] E. Björnson and E. Jorswieck, *Optimal Resource Allocation in Coordinated Multi-Cell Systems*, Foundations, T. in Communications, and I. Theory, Eds. NOW Publishing, 2013.
[35] E. Eraslan, B. Daneshrad, and C.-Y. Lou, "Performance Indicator for MIMO MMSE Receivers in the Presence of Channel Estimation Error," *IEEE Wireless Communications Letters*, vol. 2, no. 2, pp. 211–214, 2013.
[36] X. Li, E. Björnsson, E. G. Larsson, S. Zhou, and J. Wang, "Massive MIMO with Multi-cell MMSE Processing: Exploiting All Pilots for Interference Suppression," *arXiv:1505.03682v2 [cs.IT]*, May 2015.
[37] G. Fodor, P. D. Marco, and M. Telek, "On Minimizing the MSE in the Presence of Channel Information Errors," *IEEE Communications Letters*, vol. 19, no. 9, pp. 1604 – 1607, September 2015.
[38] V.-D. Nguyen, H. V. Nguyen, Y. Shin, W.-C. Lee, and O.-S. Shin, "Channel Estimation and Data Detection for Multicell Massive MIMO Systems in Correlated Channels," *Wireless Personal Communications*, no. 86, pp. 1857–1877, Dec. 2016.
[39] G. Fodor and M. Telek, "On the Pilot-Data Power Trade Off in Single Input Multiple Output Systems," *European Wireless '14*, vol. Barcelona, Spain, May 2014.
[40] M. J. Osborne, *An Introduction to Game Theory*. Oxford University Press, 2003.
[41] D. Fudenberg and J. Tirole, "Game Theory." MIT Press, 1991, ch. 1.
[42] G. Tian, "On the Existence of Equilibria in Games with Arbitrary Strategy Spaces and Preferences," *Journal of Mathematical Economics*, vol. 60, pp. 9 – 16, 2015.
[43] S. Wolfram, *The Mathematica Book, Fifth Edition*. Wolfram Research, 2003, no. ISBN: 1579550223.
[44] S. Boyd and L. Vandenberghe, *Convex optimization*, 1st ed. Cambridge University Press, 2004.